Regional Flood Frequency Analysis:
A case study in eastern Iceland

Philippe Crochet
Tinna Þórarinsdóttir

Regional Flood Frequency Analysis:
A case study in eastern Iceland

Philippe Crochet, Icelandic Met Office
Tinna Þórarinsdóttir, Icelandic Met Office

Keypage

Veðurstofa
Íslands

Report no.: VÍ 2015-007	Date.: September 2015	ISSN: 1670-8261	Public ☒ Restricted ☐ Provision:

Report title / including subtitle Regional Flood Frequency Analysis: A case study in eastern Iceland	**No. of copies:** 20 **Pages:** 47
	Managing director: Jórunn Harðardóttir
Author(s): Philippe Crochet and Tinna Þórarinsdóttir	**Project manager:** Philippe Crochet
	Project number: 4812
Project phase:	**Case number:** 2014-121

Report contracted for: Vegagerðin
Prepared in cooperation with:

Summary:

This study explores the application of the so-called index flood method, for estimating design floods at ungauged natural catchments in eastern Iceland. The method is first developed with observed flood data at available gauging stations in the region, and then with simulated flow series generated with a distributed hydrological model within gauged catchments. Results indicate that the method is applicable in the study region and capable of estimating flood quantiles with reasonable accuracy at ungauged sites.

Keywords: Iceland, flood, regional flood frequency analysis, hydrological modelling	**Managing director's signature:** **Project manager's signature:** **Reviewed by:** Davíð Egilson, Matthew J. Roberts, SG

Contents

1   Introduction

Flood frequency analysis is an important factor in flood risk assessment studies and for the design of various hydraulic structures. Often, flood quantiles estimates are required at locations where streamflow series are very short or where no data are available, making a direct flood frequency analysis impossible. Regional flood frequency analysis such as the index flood method (IFM) (Dalrymple, 1960) offers a solution to this problem and is widely used to estimate flood quantiles in these situations, see for instance Burn (1990), GREHYS (1996a, 1996b), Hosking & Wallis (1997), Jingyi & Hall (2004), Kjeldsen & D. Jones (2007), Das & Cunnane (2011), Malekinezhad *et al.* (2011a and 2011b), Zaman *et al.,* (2012) and many others. The idea is to compensate for the lack of temporal data by spatial data, taken within a homogeneous region with respect to flood characteristics, and transfer information regarding flood characteristics from gauged sites to the target site.

The IFM has already been evaluated in northern Iceland (Crochet, 2012a,b). Results are very encouraging but indicate that a limited number of gauged sites can be an obstacle to the method development. The problem of data limitation has been addressed in Crochet & Þórarinsdóttir (2014) by combining the use of the IFM with simulated streamflow series obtained with the distributed hydrological model WaSiM (Schulla & Jasper, 2007). First, WaSiM was calibrated on a gauged catchment and used to simulate streamflow series at different locations within that catchment, where no observed streamflow data were available. Then, flood statistics were extracted from these simulated series and used to develop the IFM which was used to infer flood quantiles at totally ungauged catchments located within the same region. The previous work has shown that, in principle, this combined IFM method could be developed for an entire region even if one site only was gauged, assuming that flood data were correctly simulated by the hydrological model within the gauged catchment. This report is a continuation of the work of Crochet & Þórarinsdóttir (2014).

The capacity of the IFM to estimate design floods at ungauged locations on natural catchments is now evaluated in eastern Iceland. The method is first developed with observed streamflow series at available gauging stations. Next, the method is developed with simulated streamflow series obtained with WaSiM on selected catchments, as described above. The report is organized as follows. Section 2 presents the study area and data. Section 3 describes the methodology. Section 4 presents the results of the proposed approach for estimating design floods at ungauged catchments. Finally, Section 5 concludes the report.

2   Study area and data

2.1   River basins

The region under study is located in the East fjords and the surrounding area (Fig. 1). This region is characterised by a complex topography along the coast, Vatnajökull ice cap in the southwest and highlands in the interior. This leads to large precipitation and temperature gradients in the region (Crochet *et al.,* 2007; Crochet & Jóhannesson, 2011). Eight unregulated gauged river catchments have been selected for this study. Table 1 summarizes their main characteristics.

2.2   Streamflow data

Daily flow series and monthly maximum instantaneous flow series were available at the gauging stations for variable periods (Table 1). Uncertainties related to the validity of the rating curves, used to convert observed water level into discharge, can lead to uncertainties in discharge calculations, especially for high discharge values. The daily flow series were only used for the calibration of WaSiM at selected catchments. Annual maximum flow (AMF) series were extracted for each hydrological year (1 Sept–31Aug), from the monthly maximum instantaneous flow series. Years with more than four missing months were omitted. These AMF series were used to conduct the flood frequency analysis and develop the index flood method. Figure 2 presents the time of occurrence of AMF for each catchment. One can see that for most catchments, the AMF is mainly observed between July and November, i.e mainly caused by heavy rainfall, rather than spring snowmelt.

2.3   Meteorological data

Gridded daily air temperature at 2 m above ground (Crochet & Jóhannesson, 2011) and precipitation (Crochet, 2013) calculated on a 1x1 km grid for the period 1961–2010, were used for the development of the IFM and to simulate streamflow with WaSiM. The temperature data set was obtained by gridding temperature observations at meteorological stations with a spline interpolation after elevation correction, using a fixed lapse rate of 6.5°C/km. The precipitation dataset was obtained by gridding precipitation anomaly at raingauge stations with a spline interpolation and multiplying the resulting maps with the corresponding 30-year mean monthly precipitation maps derived with an orographic precipitation model (Crochet *et al.,* 2007).

2.4   Other data

A 1x1 km digital elevation model derived from a 500 m DEM (Icelandic Meteorological Office, National Land Survey of Iceland, Science Institute, University of Iceland, and National Energy Authority. 2004), a soil map from the Agricultural University of Iceland and a vegetation map from the Icelandic Institute of Natural history were also used in this study.

Table 1. Main characteristics of river basins used in this study.

| Catchment / Gauging station	Name	Area (km^2)	Mean elevation (m a.s.l)	Mean annual precipitation (mm) (1961-2006)	Available period for streamflow data
vhm148	Fossá	116	595	2415	1969–2014
vhm149	Geithellná	190	594	2692	1971–2013
vhm205	Kelduá	269	731	1772	1977–2009
vhm206	Fellsá	128	710	1783	1977–2014
vhm221	Jökulsá í Fljótsdal	294	930	2051	1981–2014
vhm265	Hamarsá	224	679	2624	1991–2005
vhm277	Geithellnaá	100	720	2800	1992–2005
vhm278	Fossá	21	688	2246	1992–2005
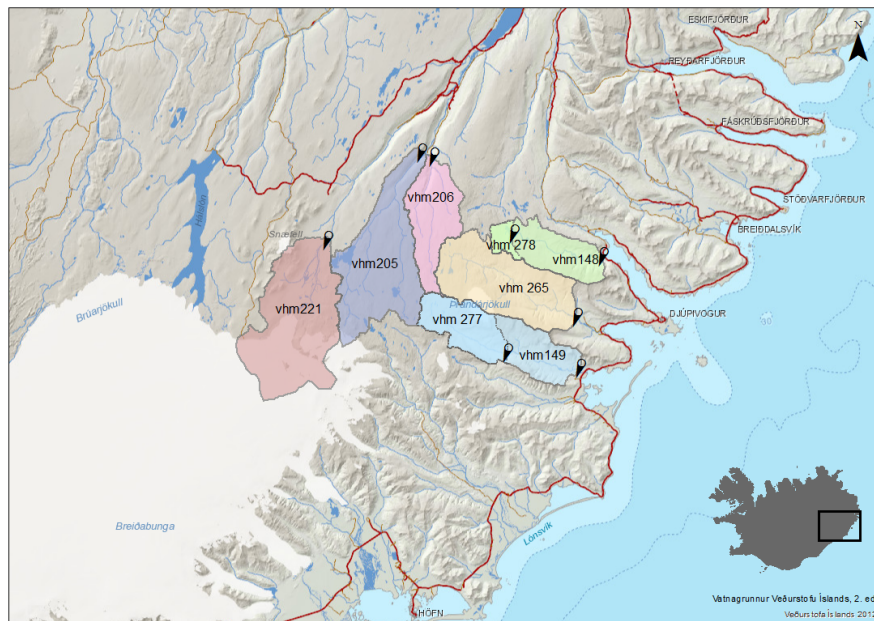
Figure 1. Region under study and location of catchments. Catchment vhm278 is embedded within vhm148 and catchment vhm277 is embedded within vhm149.
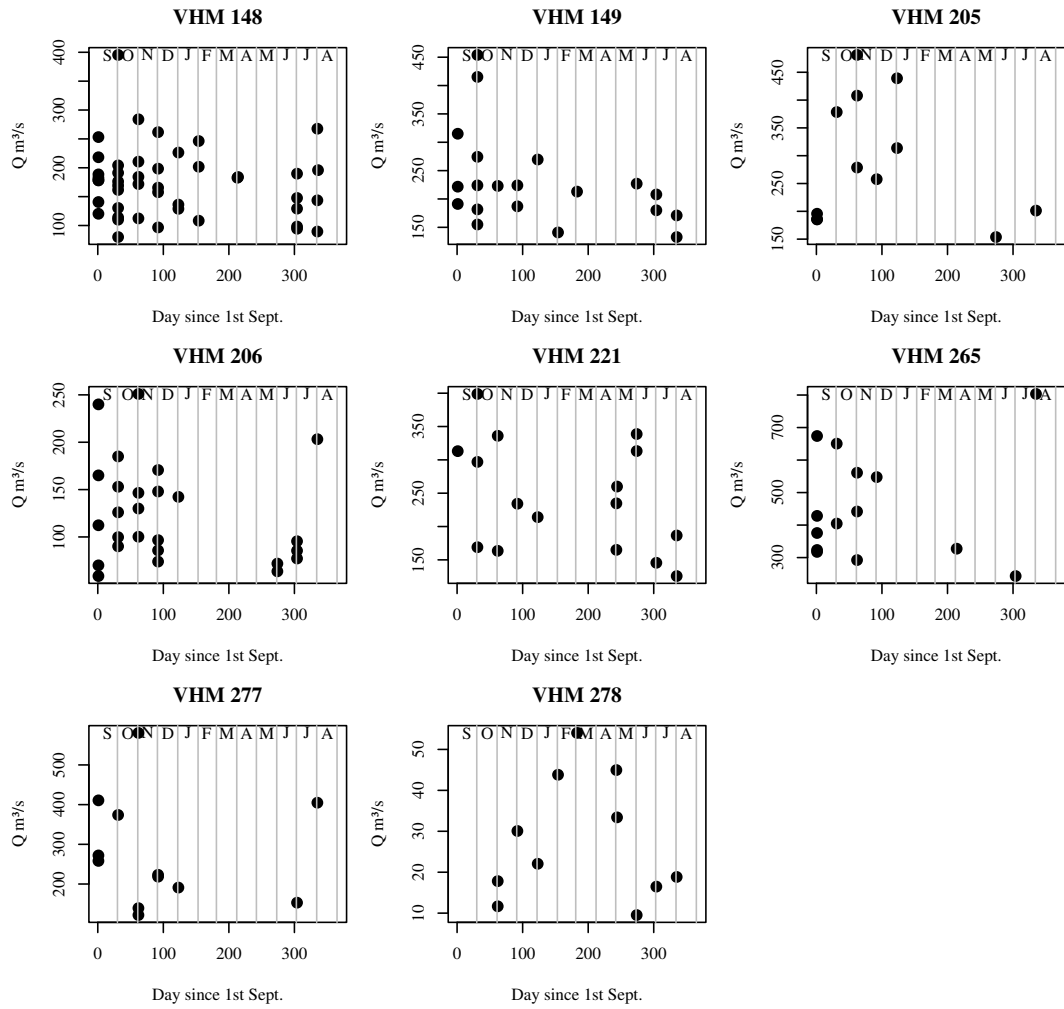
Figure 2. Time of occurrence of the annual maximum flow. For time periods, see Table 1.

3 Index flood method

3.1 General principle

The method has already been described in detail in Crochet (2012a,b) and Crochet & Þórarins-dóttir (2014) and so is only summarised here. The index flood method (IFM), proposed by Dalrymple (1960) can be used to estimate the T-year flood quantile at ungauged locations or at gauged sites with short records, using available flood data taken from gauged sites located within the same homogeneous region. These catchments are assumed to be natural and without flow alteration. The underlying assumption is that flood data within a homogeneous region are drawn from the same frequency distribution, apart from a scaling factor. The method involves two major steps: i) the identification of a group of homogeneous catchments (or a homogeneous "region") with respect to flood characteristics and ii) a regional estimation method for estimating the flood frequency distribution at each site of interest, called target site, gauged or ungauged, within the homogeneous region.

Different techniques can be used to identify homogeneous groups of catchments, i.e. catchments considered sufficiently similar to produce a similar hydrologic response with respect to extreme flow. Two methods were used in this study: i) the cluster analysis and ii) the so-called region of influence (ROI) approach (Burn 1990). With the cluster analysis, fixed homogeneous regions are obtained whereas with the ROI, a potentially unique "region", is defined for each target catchment. With both techniques, a set of physiographic and climatic catchment characteristics available at all (gauged and ungauged) catchments are defined. Then, a distance metric is used to measure the similarity of the different catchments according to these attributes. This means that streamflow data cannot be used in this step as by definition, this information is unavailable at ungauged sites. Once a homogeneous group of catchments has been preliminary identified according to the selected technique, the degree of homogeneity of the candidate "region" with respect to extreme flow statistics remains to be tested, using flood data available at the gauged sites of that region. The H-statistics, proposed by Hosking & Wallis (1993) was used here for that purpose.

Once the candidate region has been accepted as a homogeneous region, the flood frequency distribution of the target site is estimated by rescaling a dimensionless regional flood frequency distribution or growth curve, $q_R(D,T)$, common to all sites of the region, with the so-called index flood, $\mu_i(D)$, of the target site:

$$\widehat{Q}_i(D,T) = \mu_i(D)q_R(D,T), \tag{1}$$

where $\widehat{Q}_i(D,T)$ is the estimated flood quantile, i.e. the T-year flood peak discharge averaged over duration D, at site i. The regional growth curve, $q_R(D,T)$, is the ratio of $Q_i(D,T)$ to the index flood $\mu_i(D)$ and is derived by pooling the AMF series from all gauged sites belonging to the homogeneous region (see for instance Hosking *et al.,* 1985a; Hoskings & Wallis, 1997). The mean of the AMF was used in this study to define the index flood $\mu_i(D)$. If the target site is gauged, $\mu_i(D)$ can be estimated by the sample mean, whereas for ungauged target sites, $\mu_i(D)$ needs to be indirectly estimated (e.g. Brath *et al.,* 2001; Bocchiola *et al.,* 2003). This step is often performed by assuming that $\mu_i(D)$ is a function of catchment characteristics ($C_{i,k}$) (not necessarily the same ones than those used in the identification of the homogeneous region):

$$\widehat{\mu}_i(D) = f(C_{i,k}), k = 1, n. \tag{2}$$

where k denotes the kth catchment characteristic.

A power-form equation is often used:

$$\widehat{\mu}_i(D) = \theta_0 C_{i,1}^{\theta_1} C_{i,2}^{\theta_2} \dots C_{i,k}^{\theta_k} \dots C_{i,n}^{\theta_n}. \tag{3}$$

where θ_k denotes the vector of model parameters. Multiple linear regression is used to infer the model parameters after logarithm transformation (see for instance Grover *et al.,* 2002), using available information at gauged sites.

When too few gauged sites are available to develop Eq. (3), simple linear regression models can be developed by combining several catchment characteristics into one single variable (e.g. Crochet, 2012a):

$$\widehat{\mu}_i(D) = \theta_0 V_i^{\theta_1}. \tag{4}$$

where $V_i = g(C_{i,k})$ is the variable and $g()$ a function of several catchment characteristics $C_{i,k}$.

3.2   Combined IFM and hydrological modelling

When too few gauged sites are available to develop Eq. (4) and estimate the index flood $\mu_i(D)$ at ungauged sites, hydrological simulations can be used to generate streamflow series at various locations within a gauged catchment, extract the corresponding AMF series and build an index flood model (Eqs. 3 or 4) with these simulated series (see Crochet & Þórarinsdóttir, 2014).

The distributed hydrological model WaSiM (Schulla & Jasper, 2007) was used to simulate daily streamflow series at different locations within selected gauged catchments. A flood-duration-frequency (QDF) model was then used to derive flood quantiles of any duration D, $Q_i(D, T)$ from these daily streamflow simulations and develop the IFM for $D = 0$ (see Crochet, 2012c). Fig. 3 summarizes the different steps of the IFM, when it is applied with WaSiM streamflow simulations. The QDF model used here is based on the approach proposed by Javelle *et al.* (2003).

$$Q_i(D, T) = \mu_i(D) q p_i(T), \tag{5}$$

where $Q_i(D, T)$ is the T-year flood quantile at site i, averaged over duration D, $\mu_i(D)$ is the corresponding index flood, as defined above, i.e. the mean of the AMF series for duration D, and $q p_i(T)$ is a dimensionless parent distribution with mean of unity, equivalent to a growth curve. This parent distribution is estimated at each site i with the same method used to estimate $q_R(D, T)$, but instead of pooling AMF series for a given duration D from different sites, the estimation is made individually for each site i by pooling AMF series for different durations D. The index flood, $\mu_i(D)$, is modelled at each site i as a continuous function of D, as follows:

$$\mu_i(D) = \frac{\mu_i}{1 + (D/\Delta_i)^{\lambda_i}}, \tag{6}$$

where μ_i, Δ_i and λ_i are basin dependent parameters that have to be calibrated (see Crochet, 2012c). The parameter μ_i is the mean of the instantaneous AMF series, $\mu_i(D = 0)$. A regional growth curve, $q_R(D,T)$, can then be derived from the parent distributions $qp_i(T)$ obtained at all sites i belonging to the same catchment where WaSiM was used. Alternatively, the growth curve derived from the observed AMF series at the gauged site used to calibrate WaSiM can also be used to define $q_R(D,T)$. Once $\mu_i(D)$ and $q_R(D,T)$ are known for $D = 0$, the IFM can be developed to infer instantaneous flood quantiles at sites located in ungauged catchments, as described in Section 3.1.
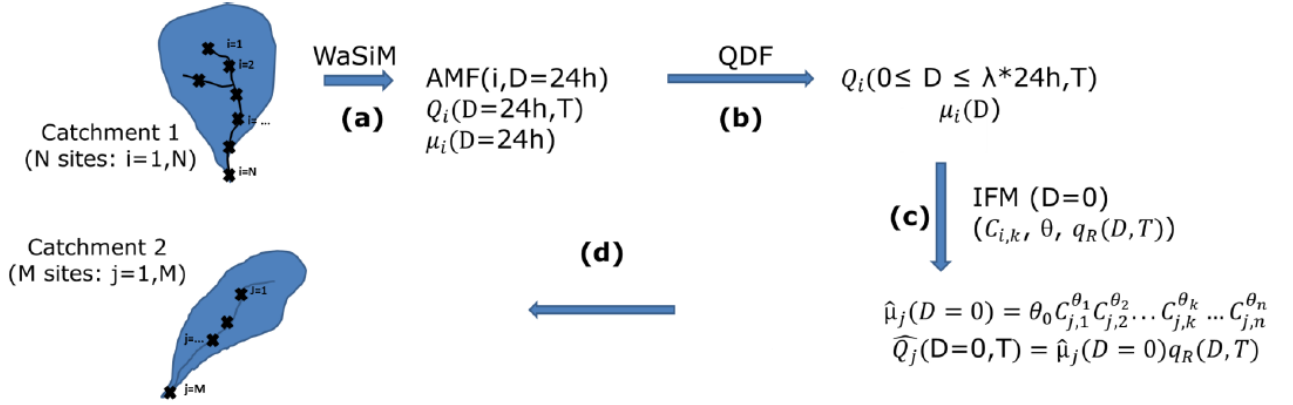

Figure 3. WaSiM-based IFM flow chart. Daily ($D = 24h$) AMF series simulated with WaSiM at specific sites within a given gauged catchment are extracted (a). A Flood-Duration-Frequency (QDF) model is applied to derive instantaneous ($D = 0$) flood quantiles and index floods (b). This information is then used to develop the IFM (c), i.e. the regional growth curve, $q_R(D,T)$, and the index flood model parameters (θ). The IFM is then used to estimate instantaneous flood quantiles at ungauged sites within catchments belonging to the same region (d).

3.3 Flood frequency distribution and parameter estimation method

The Generalized Extreme Value (GEV) distribution (Jenkinson, 1955) was adopted to model the flood frequency distribution from the AMF series:

$$Q_i(D,T) = \begin{cases} \varepsilon_i + \frac{\alpha_i}{\kappa_i}(1 - [-\ln(1 - 1/T)]^{\kappa_i}) & \text{if } \kappa_i \neq 0 \\ \varepsilon_i - \alpha_i \ln(-\ln(1 - 1/T)) & \text{if } \kappa_i = 0 \end{cases} \quad (7)$$

where ε_i is the location parameter, α_i is the scale parameter and κ_i is the shape parameter. The method of probability weighted moments (PWM) proposed by Hosking *et al.* (1985b) was adopted to fit the individual GEV distributions at each site and the parameters of the regional growth curve ($q_R(D,T)$) were estimated with the GEV/PWM regionalization algorithm proposed by Hosking *et al.* (1985a), as in Crochet (2012a,b) and Crochet & Þórarinsdóttir (2014).

3.4 Evaluation statistics

In order to assess the capacity of the IFM to estimate flood quantiles at ungauged locations, the method was developed and tested in cross-validation mode, considering instantaneous flood quantiles only ($D = 0$). Each of the eight gauged sites presented in Fig. 1 was in turn considered as the ungauged "target" site for which flood quantiles were required. The IFM was recursively developed for each target site, without using the AMF data from that site, and applied at that site, treated as ungauged. Estimated index flood and flood quantiles were then compared to the reference index flood and flood quantiles calculated with AMF observations available at the target site (see Sections 4.3.1 and 4.3.2).

The ability to predict the index flood at ungauged sites was evaluated by calculating the relative root mean squared error ($RMSE_\mu$) between reference ($\mu_i(D)$) and estimated ($\widehat{\mu_i}(D)$) index floods. The reference index flood was defined by the arithmetic mean of the observed AMF sample at the target site and the estimated index flood was obtained by Eq. (4).

$$RMSE_\mu(\%) = \sqrt{\frac{1}{N}\sum_{i=1}^{N}\left(\frac{\mu_i(D) - \widehat{\mu_i}(D)}{\mu_i(D)}\right)^2} \, x100 \quad (8)$$

Reference and estimated flood quantiles were compared at each target site, for average recurrence intervals T of 2, 5, 10, 20, 50 years. The quality of the estimation was evaluated by calculating the relative root mean squared error of the quantile estimates for each site, and then the average over all sites was calculated ($RMSE_T$):

$$RMSE_T(\%) = \frac{1}{N}\sum_{i=1}^{N}\sqrt{\frac{1}{L}\sum_{l=1}^{L}\left(\frac{Q_i(D,T_l) - \widehat{Q_i}(D,T_l)}{Q_i(D,T_l)}\right)^2} \, x100 \quad (9)$$

where $Q_i(D,T_l)$ is the reference flood quantile at gauged site i and return period T_l, calculated with the GEV distribution fitted to the observed AMF series and $\widehat{Q_i}(D,T_l)$ is the estimated flood quantile, calculated with the IFM (Eqs. 1 and 4).

4 Results

4.1 Delineation of homogeneous regions

Both cluster analysis and ROI techniques were used to identify homogeneous regions prior to applying the IFM with observed AMF series (see Section 3.1). For the cluster analysis, different clustering techniques provided by the *R* software were tested. In order to develop the index flood models (Eq. 4), six catchments at least were arbitrarily required to form a homogeneous region (excluding the target catchment). The following catchment characteristics (calculable anywhere in Iceland) were considered for the identification of these regions with both methods:

- Logarithm of catchment area ($Log(A)$)

- Mean catchment altitude (Z)

- Catchment perimeter (L)

- Ratio between actual catchment area and area of circular catchment of perimeter L

- Percentage of glaciated area (G)

- Mean annual precipitation (1961-2006) (P)

- Mean annual maximum snowpack (1961-2006) (SWE_m)

- Mean annual maximum daily input water supply (1961-2006) (WS_m)

- Normalized mean monthly input water supply (1961-2006) ($NWS(j), j = 1,..,12$)

- Mean snow cover fraction on May 1st (1961-2006) (SCF)

- Logarithm of saturated hydraulic conductivity ($Log(K_s)$)

Daily precipitation was split into rain or snow according to a temperature threshold. A simple temperature-index melt model that relates air temperature to snow and ice melt rates was used to estimate the snowpack evolution and glacier melt. Input water supply was estimated as the sum of rain and snowmelt (and ice melt). Fig. 4 presents the normalized mean daily input water supply and discharge seasonalities. The normalisation is defined by dividing each series by its respective mean. The normalized mean discharge seasonality is well described by the seasonality of the normalized mean input water supply. This indicates that the input water supply can be used to capture some insights into the hydrological characteristics of the catchments of the region.

Fig. 5 presents the dendrograms showing the hierarchy among catchments according to the cluster analysis. Different groups emerge, depending on the specific technique used. All results indicate that vhm221 stands out, while the other catchments define a more homogeneous group. This is not surprising as vhm221 is located in the interior of the region and is 50% glaciated. For sake of simplicity, it was decided to form one single candidate region with all catchments, according to the cluster analysis. Table 2 presents the homogeneous groups of catchments obtained with the ROI technique, associated to each target catchment. The catchments are ordered from most similar to least similar.
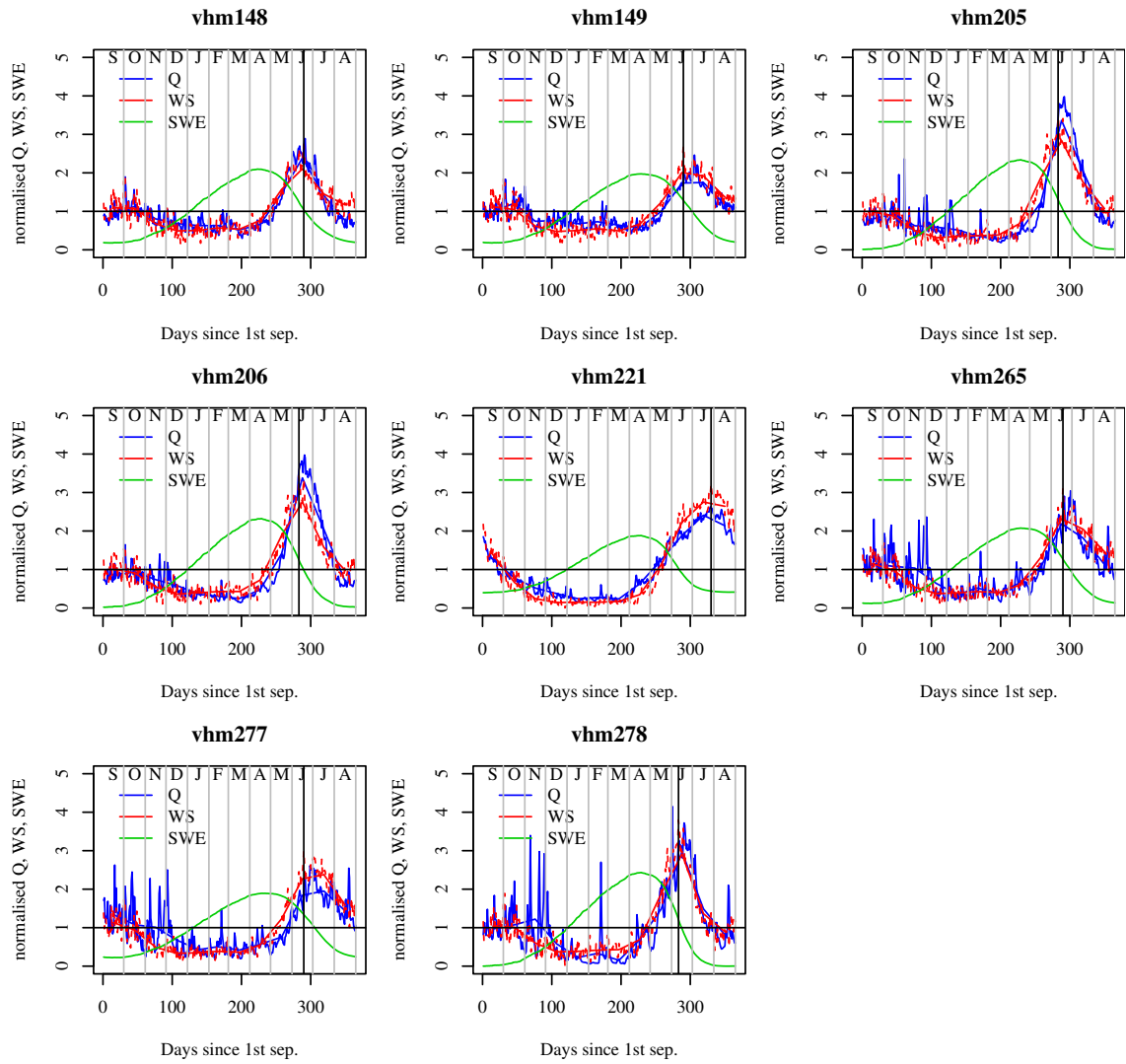
15

Figure 4. Normalized mean input water supply (WS), mean discharge (Q) and mean snow-pack (SWE) seasonality.
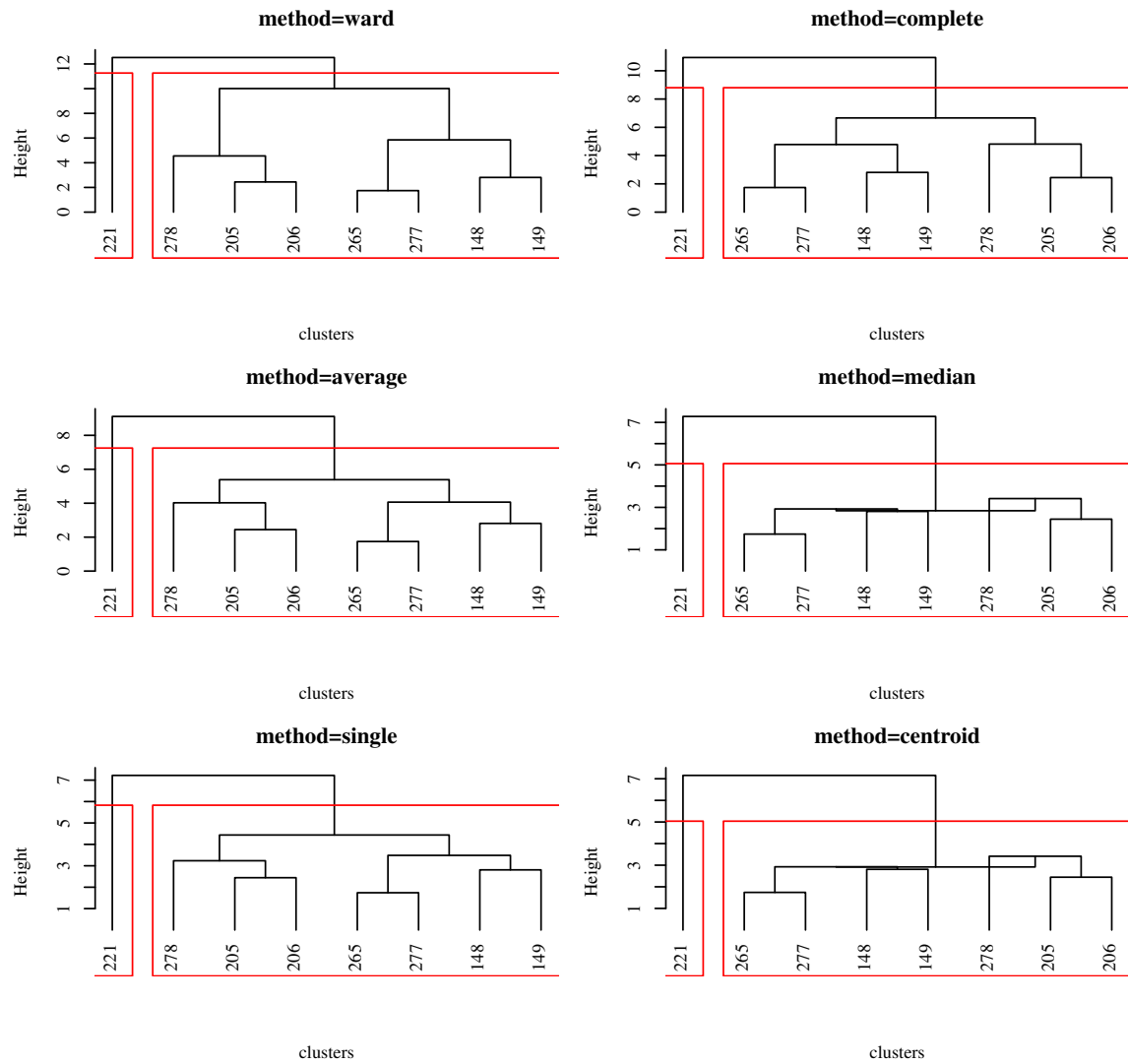
Figure 5. Cluster analysis using six different methods. Numbers on the x-axis correspond to gauging station number, see Table 1.

Table 2. ROI technique: homogeneous groups of catchments associated to each target catchment.

Target catchment	ROI
vhm148:	vhm149, vhm265, vhm278, vhm206, vhm277, vhm205
vhm149:	vhm148, vhm265, vhm277, vhm206, vhm278, vhm205
vhm205:	vhm206, vhm278, vhm265, vhm277, vhm148, vhm149
vhm206:	vhm205, vhm278, vhm148, vhm265, vhm277, vhm149
vhm221:	vhm277, vhm265, vhm205, vhm206, vhm278, vhm149
vhm265:	vhm277, vhm149, vhm148, vhm206, vhm278, vhm205
vhm277:	vhm265, vhm149, vhm148, vhm278, vhm206, vhm205
vhm278:	vhm206, vhm148, vhm265, vhm205, vhm277, vhm149

4.2 Regional growth curves

The validity of the candidate regions identified by cluster analysis and ROI technique was verified by studying the homogeneity of the associated regional growth curves derived from observed AMF series, through the calculation of the H-statistics (Hosking & Wallis, 1993). The growth curves associated to the region defined by cluster analysis (i.e. all catchments) are presented in Fig. 6. Table 3 gives the H-statistics obtained after excluding one catchment at the time (target catchment). The H-statistics confirm that all eight catchments can be considered sufficiently homogeneous to form a single region ($H < 2$). A first IFM (IFM-CLU) was defined using one single homogeneous region identified by cluster analysis, and all available observed AMF series (excluding the target site). Table 4 presents the H-statistics obtained when the ROI method was used to define homogeneous groups of catchments, with and without target site. Appendix I presents the corresponding growth curves. Results confirm the homogeneity of the ROI-based homogeneous regions with respect to flood statistics. A second IFM (IFM-ROI) was defined with observed AMF series corresponding to gauged sites identified by the ROI technique.

Table 3. Cluster analysis: H-statistics without target catchment.

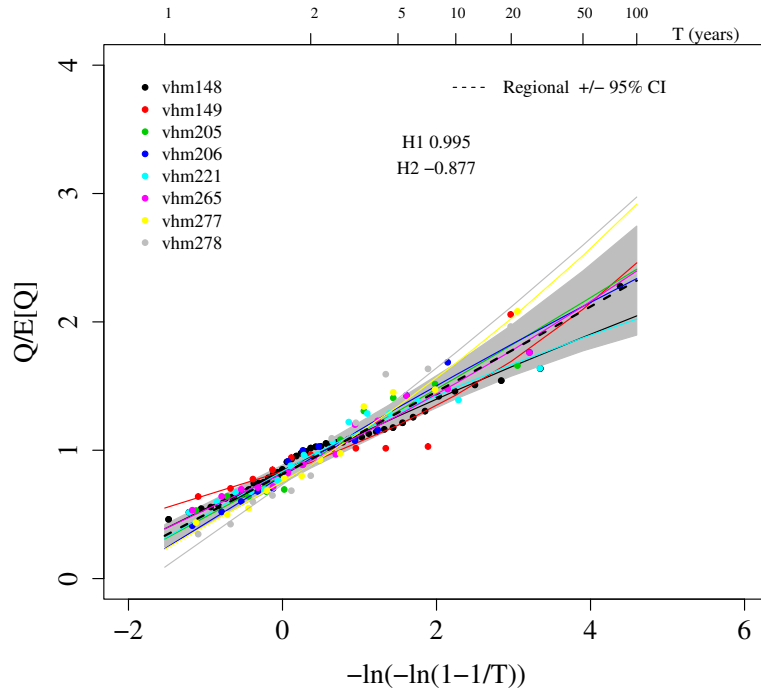|	H-statistics
Target catchment	without target catchment
vhm148	0.95
vhm149	1.46
vhm205	1.01
vhm206	1.28
vhm221	0.9
vhm265	1.16
vhm277	0.87
vhm278	-0.12

18

Figure 6. Individual and regional growth curves from the homogeneous region defined by cluster analysis. Grey region corresponds to the 95% confidence interval of the regional growth curve.

Table 4. H-statistics associated to the ROI of each target catchment.

Target catchment	H-statistics without target catchment	H-statistics with target catchment
vhm148	0.52	0.84
vhm149	1.45	0.91
vhm205	0.91	0.84
vhm206	1.14	0.89
vhm221	0.57	0.85
vhm265	1	0.91
vhm277	0.91	0.87
vhm278	-0.14	0.87

4.3   WaSiM model simulations

Results from the cluster analysis mean that in principle, any of the eight catchments used in the study can be selected to estimate the regional growth curve of that region, if a long enough AMF series is available at the gauging site in question. WaSiM was used to simulate long daily discharge series at different locations within three selected gauged catchments (vhm148, vhm149, and vhm206) and AMF series were extracted.

First, a multi-objective calibration method was used to calibrate WaSiM, as in Crochet (2014), but with an objective function more adapted to the simulation of AMF. A set of seven model parameters were calibrated: 1) recession constant of direct runoff, 2) drainage density, 3) satu-

rated hydraulic conductivity, 4) temperature threshold for snowmelt, 5) temperature dependent melt factor, 6) fraction of snowmelt which is direct flow and 7) storage capacity of snow for water (see Schulla & Jasper, 2007). The recession constant of interflow was arbitrarily set to the recession constant of direct runoff. Other parameters were fixed according to previous studies. An ensemble of 500 parameter-sets was formed by randomly generating the values of each parameter from a uniform distribution. The corresponding 500 model runs were completed for the calibration period, including a spin-up period of three years. Each model setup was then ranked from worst to best according to the following criteria:

1. $NS-AMF$: worst=Min($NS-AMF$); best=Max($NS-AMF$)

2. $NS-Q_d$: worst=Min($NS-Q_d$); best=Max($NS-Q_d$)

3. $NS-E[Qd]$: worst=Min($NS-E[Qd]$); best=Max($NS-E[Qd]$)

Where NS is the Nash-Sutcliffe efficiency (Nash & Sutcliffe, 1970) applied to AMF, daily discharge (Q_d) and discharge seasonality (i.e. mean discharge on each calendar day, $E[Qd]$).

Then, a weighted rank was calculated and each model setup sorted accordingly:

$$WR = 0.5\text{Rank}(NS-AMF) + 0.3\text{Rank}(NS-Q_d) + 0.2\text{Rank}(NS-E[Qd]) \qquad (10)$$

Next, the best model run was selected and validated on a different period than the calibration period. Results of the calibration and validation periods are summarized in Tables 5 and 6 and Appendix II. Overall, WaSiM model simulations compare quite well with observations. Discharge resulting from spring snowmelt was generally well simulated, but some discrepancies were observed in some years in late spring or early summer, due to a snowpack under estimation. The magnitude of annual maximum daily flow was often underestimated, especially at vhm148 and vhm206, partly because of difficulties to capture flood-triggering precipitation, partly because of modelling uncertainties and partly because of uncertainties in the rating curves for the most extreme discharge values. The best model parameterisation identified in the calibration period was found to be similarly acceptable in the validation phase and selected to conduct the hydrological simulations on the three catchments. Daily discharge series were then simulated at different locations on the three catchments (Fig. 7), over the period 1961-2006 for vhm148 and vhm149 and 1961-2010 for vhm206.

Instantaneous AMF statistics were derived by QDF modelling of the simulated daily AMF series (see Appendix 3). The underestimation of daily AMF with WaSiM led to the underestimation of instantaneous AMF statistics ($\mu_i(D=0)$ and $Q_i(D=0,T)$) at vhm148 and vhm206, whereas $\mu_i(D=0)$ and $Q_i(D=0,T)$ were observed to be within the reference 95% confidence interval (CI) for vhm149. Therefore, simulations made within vhm149 only were used to develop the IFM based on WaSiM (IFM-WaSiM), to be applied in the region. The regional growth curves derived from IFM-CLU, IFM-ROI and IFM-WaSiM are presented in Fig. 8. One can see that the regional growth curve derived from WaSIM is relatively close to the ones derived from observed AMF series.
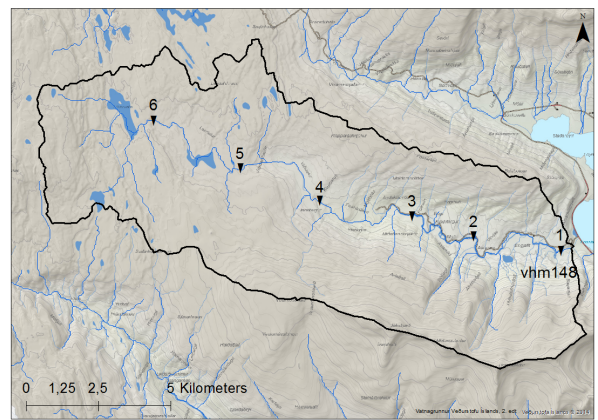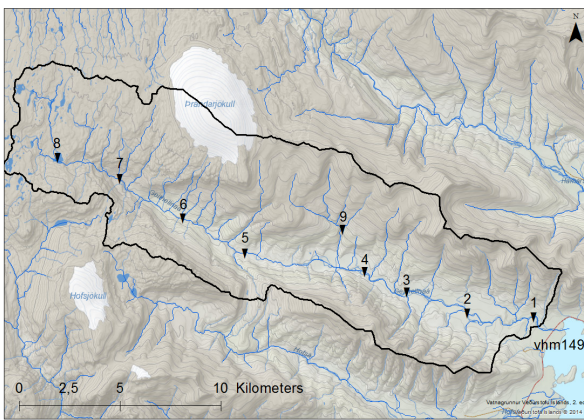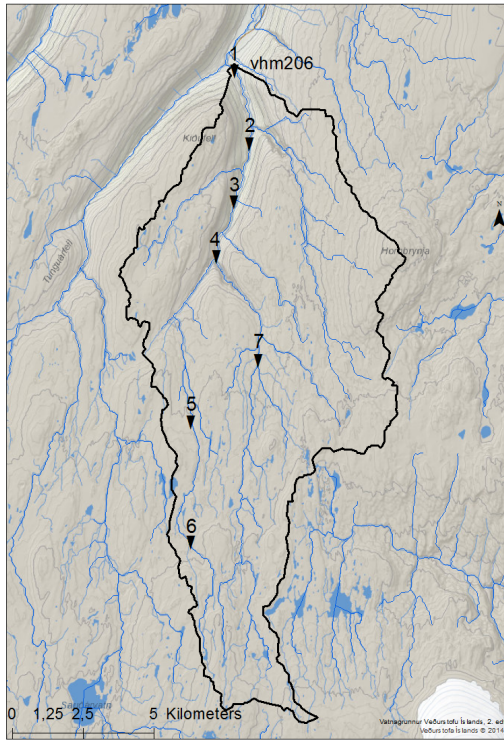
Figure 7. Location of simulated sites within catchments vhm206 (top), vhm149 (bottom-left) and vhm148 (bottom-right).

Table 5. Verification of WaSiM simulations in the calibration period.

Gauging station	vhm148	vhm149	vhm206
NS (daily discharge)	0.624	0.541	0.53
Mean error (daily discharge) (m^3/s)	–0.81	-2.1	–0.82
Mean error (annual discharge) (m^3/s)	–0.81	-2.2	–0.73
Mean error (AMF) (m^3/s)	–34.6	–19.5	-31.7

Table 6. Verification of WaSiM simulations in the validation period.

Gauging station	vhm148	vhm149	vhm206
NS (daily discharge)	0.456	0.453	0.452
Mean error (daily discharge) (m^3/s)	–1	–6	–0.62
Mean error (annual discharge) (m^3/s)	–0.95	–6.4	–0.52
Mean error (AMF) (m^3/s)	–20.4	–30.1	–14.7
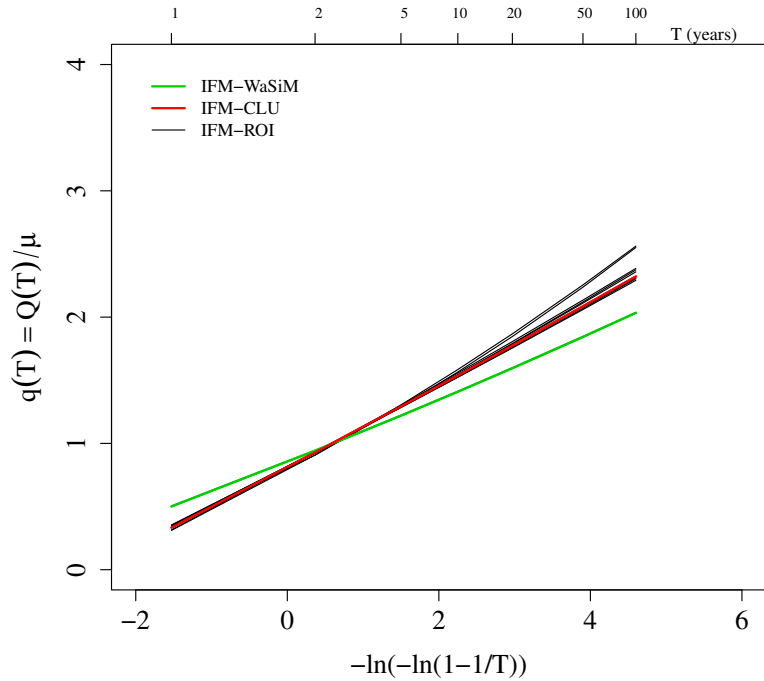
Figure 8. Regional growth curves derived from cluster analysis (IFM-CLU) and from the ROI associated to each catchment (IFM-ROI), using observed AMF series, and from WaSiM simulations made within catchment vhm149 (IFM-WaSiM).

4.3.1 Index flood modelling

Twelve relationships between the index flood, $\mu_i(D=0)$, and various physiographic and climatic catchment characteristics were defined in order to estimate the index flood at ungauged sites ($\widehat{\mu}_i(D=0)$). Given the few gauged sites available in the region, the models were defined by combining several characteristics into one single variable (cf. Eq. 4). The model parameters were estimated by ordinary least squares (OLS) regression after logarithmic transformation:

$$\text{model no. 1:} \qquad \widehat{\mu}_i(D=0) = \theta_0 (A_i)^{\theta_1} \tag{11}$$

$$\text{model no. 2:} \qquad \widehat{\mu}_i(D=0) = \theta_0 (L_i)^{\theta_1} \tag{12}$$

$$\text{model no. 3:} \qquad \widehat{\mu}_i(D=0) = \theta_0 (A_i/L_i)^{\theta_1} \tag{13}$$

$$\text{model no. 4:} \qquad \widehat{\mu}_i(D=0) = \theta_0 (A_i/Z_i)^{\theta_1} \tag{14}$$

$$\text{model no. 5:} \qquad \widehat{\mu}_i(D=0) = \theta_0 (A_i P_i)^{\theta_1} \tag{15}$$

$$\text{model no. 6:} \qquad \widehat{\mu}_i(D=0) = \theta_0 (A_i P_i/Z_i)^{\theta_1} \tag{16}$$

$$\text{model no. 7:} \qquad \widehat{\mu}_i(D=0) = \theta_0 (A_i P_i/L_i)^{\theta_1} \tag{17}$$

$$\text{model no. 8:} \qquad \widehat{\mu}_i(D=0) = \theta_0 (A_i P_i/(Z_i L_i))^{\theta_1} \tag{18}$$

$$\text{model no. 9:} \qquad \widehat{\mu}_i(D=0) = \theta_0 (A_i P_{mi})^{\theta_1} \tag{19}$$

$$\text{model no. 10:} \qquad \widehat{\mu}_i(D=0) = \theta_0 (A_i P_{mi}/Z_i)^{\theta_1} \tag{20}$$

$$\text{model no. 11:} \qquad \widehat{\mu}_i(D=0) = \theta_0 (A_i R_{mi})^{\theta_1} \tag{21}$$

$$\text{model no. 12:} \qquad \widehat{\mu}_i(D=0) = \theta_0 (A_i R_{mi}/Z_i)^{\theta_1} \tag{22}$$

Where $\theta = (\theta_0, \theta_1)$ is the vector of regression parameters, i is the catchment index, P_m the catchment averaged annual maximum daily precipitation for the period 1961–2006, and other catchment characteristics are defined in Section 4.1. Models no. 1–4 (Eqs. 11–14) include physiographic catchment characteristics only, whereas models no. 5–12 (Eqs. 15-22) combine physiographic and climatic characteristics.

In total, three sets of twelve models were developed and then used to estimate $\mu_i(D=0)$ at each of the eight gauged sites (cf. Fig. 1), recursively treated as ungauged, and for which the catchment characteristics are known (see Section 3.4). The first set was developed using the homogeneous region identified by cluster analysis (IFM-CLU). The second set was developed using the homogeneous regions identified by ROI (IFM-ROI) (cf. Table 2). These two set of models were calibrated with the index flood $\mu_i(D=0)$ calculated by the sample mean of observed AMF series. The third set of models (IFM-WaSiM) was calibrated with the index flood $\mu_i(D=0)$ derived by QDF modelling of simulated AMF series within catchment vhm149. IFM-CLU and IFM-ROI were recursively developed without using any information from the target site in question, treated as ungauged. IFM-WaSiM was developed once for all with all simulated sites within vhm149, so that when IFM-WaSiM is applied at gauged site vhm149, this site cannot be considered ungauged.

Figs. 9–12 summarize the results of the comparison between reference and estimated index floods. The reference index flood is defined by the arithmetic mean of the observed AMF sample.

23

For each IFM set, one can see that several index flood models perform relatively similarly (Fig. 9). One can also see that for each set, there usually is one model at least providing an acceptable estimate of $\mu_i(D=0)$ for each catchment, i.e. close to or within the 95% CI of $\mu_i(D=0)$. However, as one cannot know a-priori which model will perform best at ungauged catchments, one of the twelve models has to be selected a-priori on the basis of results obtained at gauged catchments, through the cross-validation procedure.

Different factors can contribute to a poor index flood model, leading to poor estimates of $\mu_i(D=0)$ at ungauged catchments. Firstly, the model may be inappropriate to describe the spatial variations of $\mu_i(D)$ in the region under study. Secondly, the degree of hydrological similarity between the target catchment and the homogeneous region is too poor. Thirdly, the index flood model is applied to a catchment whose characteristics are beyond the range of characteristics for which the model was developed. Finally, sampling variability can affect the quality of the index flood model. As an illustration, $\mu_i(D=0)$ was calculated for vhm148 considering 15-year moving windows (Fig. 10). The effect of sampling variability on the estimation of $\mu_i(D=0)$ appears very clearly. The observed AMF series at the eight gauged sites are of different lengths and do not always overlap in time, which adds uncertainty to $\mu_i(D=0)$ and to the models development and therefore their validity.

The best index flood model is different for each IFM set (Fig. 11). According to the relative RMSE ($RMSE_\mu$), the best IFM-CLU is no. 11 (Eq. 21) ($RMSE_\mu = 52\%$), the best IFM-ROI is no. 5 (Eq. 15) ($RMSE_\mu = 44\%$), and the best IFM-WaSiM is no. 4 (Eq. 14) ($RMSE_\mu = 31\%$). Overall, the best results are obtained with IFM-WaSiM, followed by IFM-ROI and IFM-CLU. In other words, the IFM developed with simulated series performs slightly better than the ones developed with observed AMF series.

When the best index flood model is considered for IFM-CLU and IFM-ROI, respectively, results indicate that $\widehat{\mu}_i(D=0)$ is usually within or close to the 95% CI of the reference $\mu_i(D=0)$ for catchments vhm148, vhm205, vhm206, vhm265 and relatively biased for catchments vhm149, vhm221, vhm277 and vhm278. Catchment vhm221 is the largest and highest and appeared relatively isolated from the others in the cluster analysis, which could explain the difficulty for the different models to estimate $\mu_i(D=0)$ at that site with available information at other sites. The poor estimation at vhm149 by most models cannot be explained by the fact that catchment characteristics are out of range. This result could be related to sampling variability discussed above. For this catchment, AMF data are available for the period 1971–1981, whereas for the other catchments, AMF data are available after 1988. Note also that the H-statistics obtained for the ROI of vhm149 is the highest (cf. Table 4), which could indicate potential heterogeneity with respect to flood statistics and partly explain the difficulty of estimating $\mu_i(D=0)$ with the IFM at that site. Estimates obtained with IFM-WaSiM are relatively unbiased at most catchments except at vhm265 and vhm277. Fig. 12 presents the scatter plot of $\mu_i(D=0)$ vs. $\widehat{\mu}_i(D=0)$ obtained with the best index flood model of each IFM-set.
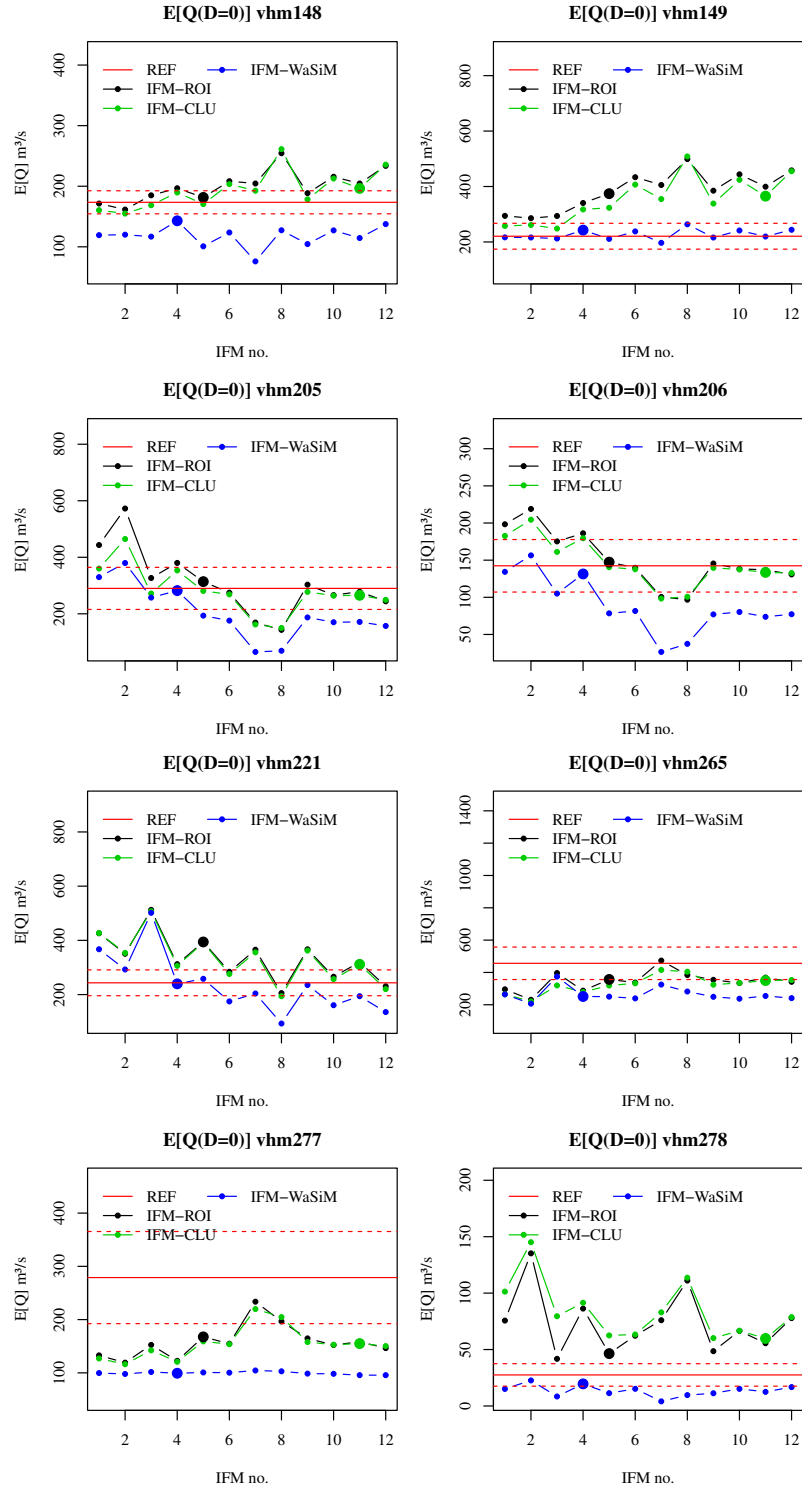
Figure 9. Index flood estimation, $\widehat{\mu}_i(D = 0)$, at each gauged site treated as ungauged, using models 1–12 (Eqs. 11–22). The solid red line corresponds to the reference index flood, estimated as the arithmetic mean of the observed AMF sample and the dashed red lines the 95% CI. Large symbols indicate overall best model for each IFM set.
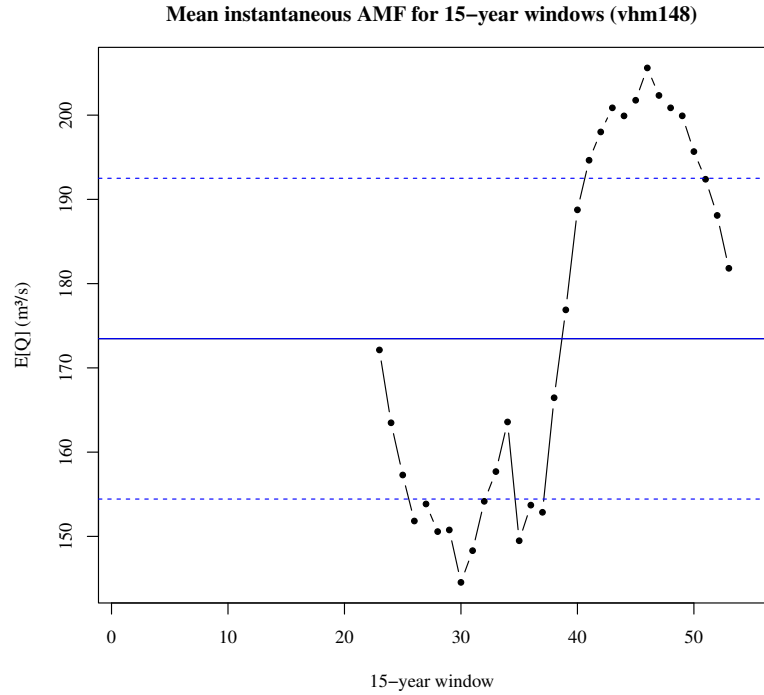
Mean instantaneous AMF for 15−year windows (vhm148)

Figure 10. Effect of sampling variability for the estimation of $\mu_i(D = 0)$ at vhm148, considering 15-year moving windows (black line). The solid blue line corresponds to $\mu_i(D = 0)$ estimated on the entire AMF sample and the dashed blue lines the 95% CI.
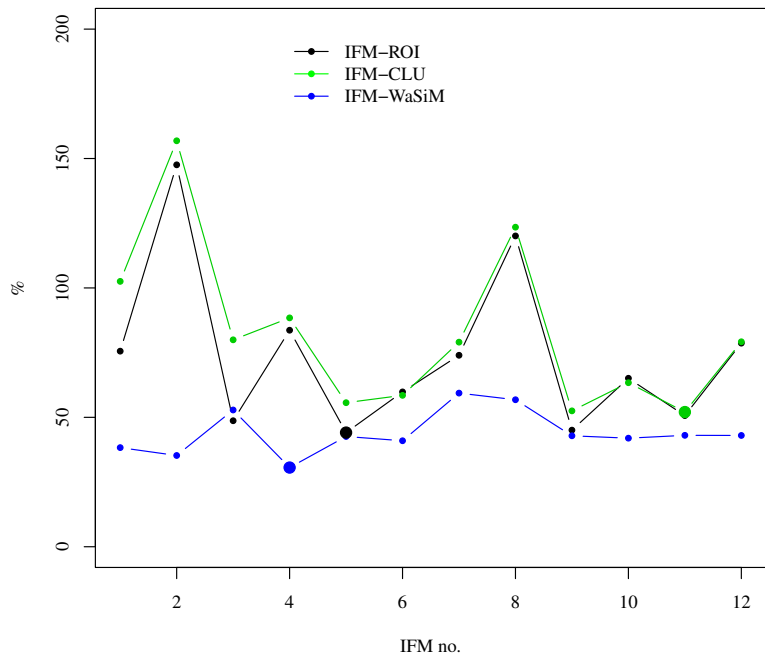
Figure 11. Estimation of $\mu_i(D = 0)$ at ungauged sites: relative RMSE ($RMSE_\mu$) for the different IFM sets and corresponding twelve index flood models (Eqs. 11–22). Large symbols indicate best model for each IFM set.
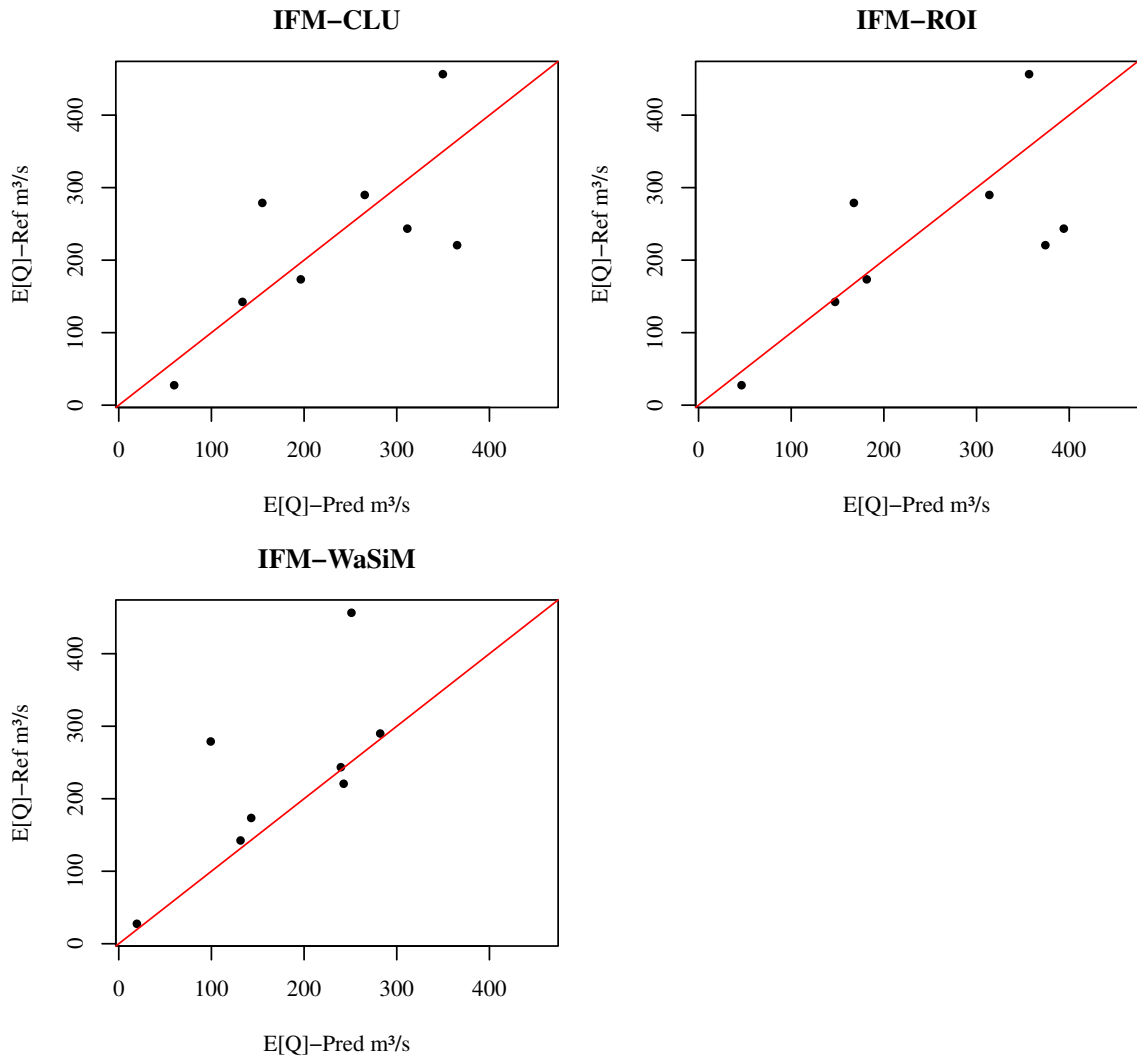
Figure 12. Index flood estimation using best index flood model for each set: $\mu_i(D = 0)$ vs. $\widehat{\mu}_i(D = 0)$. Solid red line corresponds to the 1:1 line. Top-left: IFM-CLU with model no. 11. Top-right: IFM-ROI with model no. 5. Bottom-left: IFM-WaSiM with model no. 4.

4.3.2 Flood quantiles estimation

The different variations of the IFM proposed in this study, i.e. IFM-CLU, IFM-ROI and IFM-WaSiM, developed with twelve index flood models (Eq. 11–22), were used to estimate instantaneous flood quantiles at each target site treated as ungauged. The relative RMSE ($RMSE_T$, see Section 3.4) calculated on five quantiles (T=2, 5, 10, 20 and 50 years) summarizes the overall quality of these estimates (Fig. 13) and gives a comparison of their respective performances. According to $RMSE_T$, the best results are obtained with index flood model no. 5 (Eq. 15) when IFM-ROI is applied, index flood model no. 9 (Eq. 19) when IFM-CLU is applied and index-flood model no. 4 (Eq. 14) when IFM-WaSiM is applied. The best overall results are obtained with IFM-WaSiM applied with index-flood model no. 4 (Eq. 14). The flood quantile estimation error depends on the quality of: i) the index flood model (Eqs. 11–22), ii) the regional growth curve, $q_R(D = 0, T)$, and iii) the hydrological simulations made within vhm149, for IFM- WaSiM. As a consequence, the best results are not systematically obtained with the best index flood model (see Fig. 11 and Fig. 13 for a comparison), because of compensating errors such as an over- (under-) estimation of the catchment growth curve ($q_i(D, T)$) by the regional growth curve ($q_R(D, T)$) and an under- (over-) estimation of the index flood ($\mu_i(D = 0)$) by the index flood model. However, the dominating source of error is often the quality of $\widehat{\mu}_i(D = 0)$. Appendix IV presents the reference and estimated flood frequency distributions obtained at each gauged site, treated as ungauged, considering the best index flood models for IFM-ROI, IFM-CLU and IFM-WaSiM respectively (see Fig. 11). When these models are used, the estimated quantiles are relatively unbiased in average and are usually within the 95% CI of the reference quantiles in a majority of target sites. Poor quantile estimates are obtained for catchments where $\widehat{\mu}_i(D = 0)$ is most biased. The corresponding $RMSE_T$ varies between 28% of the reference quantiles with IFM-WaSiM to 39% with IFM-CLU (Fig. 13).
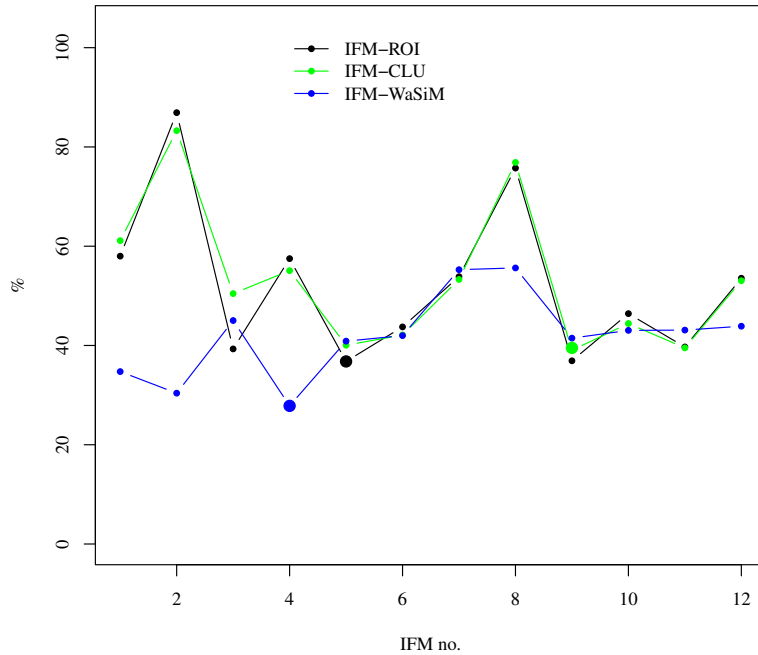
Figure 13. Estimated instantaneous flood quantiles with the IFM, at gauged sites treated as ungauged. Mean relative quantile RMSE ($RMSE_T$) for the different IFM sets and corresponding twelve index flood models (Eqs. 11–22). Large symbols correspond to the model giving the best results for each set.

5 Conclusion and future research

Lack of data is the most difficult challenge that hydrologists and engineers face in the design of hydraulic structures. The IFM offers a solution to this problem by pooling flood data from different gauged sites belonging to a homogeneous region, in order to estimate flood quantiles at ungauged locations or at gauged sites where streamflow series are very short. The primary goal of this study was to test the applicability of the IFM in the East fjords and the surrounding area, using available streamflow data. Results are conclusive and indicate the potential for this method in that region when design floods are required on catchments with no known flow alteration.

However, the development of a robust method is challenging when few gauged sites are available or when sampling variability affects the method development, because flood data from different sites do not correspond to the same period. For this reason, a secondary goal was to investigate the possibility to develop the IFM with simulated streamflow series obtained with the distributed hydrological model WaSiM, followed by QDF modelling. This hybrid method could offer an alternative solution for estimating flood quantiles in regions where the limited number of gauged sites could prevent the development of the IFM with streamflow observations. In principle, this method could be developed for an entire region even if one site only was gauged. This scenario was tested in this study, similar to what was done in northern Iceland (Crochet & Þórarinsdóttir, 2014). Results indicated the difficulty to simulate AMF with WaSiM for two of the tested catchments. The best AMF simulations were obtained within vhm149 and the IFM was developed with these data (IFM-WaSiM). This method gave slightly better results than those obtained with the IFM developed with observed AMF series (IFM-CLU and IFM-ROI). The drawback of using WaSiM however is the additional data requirement and effort needed to calibrate the

29

hydrological model, so this solution is more to be used if observed AMF series are too few to develop the traditional IFM.

Whether the IFM is developed with observed or simulated series, the main difficulty is related to the estimation of the index flood $\mu_i(D)$ for catchments whose characteristics are far outside the range of characteristics used to develop the index flood model. In such a case, the model is extrapolated beyond the range for which it was developed and the index flood estimate, $\widehat{\mu_i}(D)$, may be quite uncertain. An important under- or over-estimation of $\mu_i(D)$ will have a strong impact on the estimated flood quantiles $\widehat{Q}_i(T)$, even if the regional growth curve is well estimated and representative for the catchment of interest.

The IFM methodology needs to be further assessed in other regions, with different geological environments and flow regimes. Furthermore, more effort needs to be made in improving flood simulations with WaSiM. Finally, the assessment of the uncertainties associated to the hydrological modelling and the QDF modelling and their inclusion into the calculation of the flood quantile uncertainty needs to be investigated.

6 Acknowledgements

7 References

Bocchiola, D., De Michele, C. & Rosso, R. (2003). Review of recent advances in index flood estimation. Hydrol. Earth Sys. Sci., 7(3), 283–296.

Brath, A., Castellarin, A., Franchini, M. & Galeati, G. (2001). Estimating the index flood using indirect methods. Hydrol. Sci. J., 46(3), 399–418.

Burn, D.H. (1990). Evaluation of regional flood frequency analysis with a region of influence approach. Water Resour. Res., 26(10), 2257–2265.

Crochet, P. (2012a). Estimating the flood frequency distribution for ungauged catchments using an index flood procedure. Application to ten catchments in Northern Iceland. Icelandic Met. Office report No. VÍ 2012-005, 59pp.

Crochet, P. (2012b). Evaluation of two delineation methods for regional flood frequency analysis in northern Iceland. Icelandic Met. Office report No. VÍ 2012-013, 55pp.

Crochet, P. (2012c). Flood-duration-frequency modelling. Application to ten catchments in Northern Iceland. Icelandic Met. Office report No. VÍ 2012-006, 50pp.

Crochet, P. (2013). Gridding daily precipitation with an enhanced two-step spatial interpolation method. Icelandic Met. Office technical report No. PC/2013-01, 26pp.

Crochet, P. (2014). Probabilistic daily streamflow forecasts based on the combined use of a hydrological model and an analogue method. Icelandic Met. Office report No. VÍ 2014-006, 68pp.

Crochet, P. & Jóhannesson, T. (2011). A data set of gridded daily temperature in Iceland, 1949–2010. Jökull, 61, 1–17.

Crochet, P. & Þórarinsdóttir, T. (2014). Flood frequency estimation for ungauged catchments in Iceland by combined hydrological modelling and regional frequency analysis. Icelandic Met. Office report No. VÍ 2014-001, 50pp.

Crochet, P., Jóhannesson, T., Jónsson, T., Sigurðsson, O., Björnsson, H., Pálsson, F. & Barstad, I. (2007). Estimating the spatial distribution of precipitation in Iceland using a linear model of orographic precipitation. J. Hydrometeorol., 8, 1285–1306.

Dalrymple, T. (1960). Flood frequency analysis. US Geol. Surv. Water Supply Paper, 1543 A.

Das, S. & Cunnane, C. (2011). Examination of homogeneity of selected Irish pooling groups. Hydrol. Earth Sys. Sci., 15, 819–830.

GREHYS. (1996a). Presentation and review of some methods for regional flood frequency analysis. J. Hydrol., 186, 63–84.

GREHYS. (1996b). Inter-comparison of regional flood frequency procedures for Canadian rivers. J. Hydrol., 186, 85–103.

Grover, P.L., Burn, D.H. & Cunderlik, J.M. (2002). A comparison of index flood estimation procedures for ungauged catchments. Can. J. Civ. Eng., 29, 731–741.

Hoskings, J.R.M. & Wallis, J.R. (1993). Some statistics useful in regional frequency analysis. Water. Resour. Res. 29, 271-281.

Hosking, J.R.M. & Wallis, J.R. (1997). Regional frequency analysis. An approach based on L-Moments. Cambridge University Press. 224pp.

Hosking, J.R.M., Wallis, J.R. & Wood, E.F. (1985a). An appraisal of the regional flood frequency procedure in the UK Flood Studies Report. Hydrol. Sci. J., 30, 85–109.

Hosking, J.R.M., Wallis, J.R. & Wood, E.F. (1985b). Estimation of the generalized extreme-value distribution by the method of the probability-weighted moments. Technometrics, 27(3), 251–261.

Javelle, P., Ouarda, T.B.M.J. & Bobée, B. (2003). Spring flood analysis using the flood-duration-frequency approach: Application to the provinces of Quebec and Ontario, Canada. Hydrol. Proc., 17, 3717–3736.

Jenkinson, A.F. (1955). The frequency distribution of the annual maximum (or minimum) of meteorological elements. Quart. J. R. Met. Soc. 81, 158–171.

Jingyi, Z. & Hall, M.J. (2004). Regional flood frequency analysis for Gan-Ming river basin in China. J. Hydrol., 296, 98–117.

Kjeldsen, T.R. & Jones, D. (2007). Estimation of an index flood using data transfer in the UK. Hydrol. Sci. J., 52(1), 86–98.

Malekinezhad, H., Nachtnebel, H.P. & Klik, A. (2011a). Comparing the index flood and multiple-regression methods using L-moments. J. Phys. Chem. Earth, 36, 54–60.

Malekinezhad, H., Nachtnebel, H.P. & Klik, A. (2011b). Regionalization approach for extreme flood analysis using L-moments. J. Agr. Sci. Tech., 13, 1183–1196.

Nash, J., & Sutcliffe, J. (1970). River flow forecasting through conceptual models I: A discussion of principles. J. Hydrol., 10, 282-290.

R. Development Core Team 2010. R: A language and environment for statistical computing. R Foundation for Statistical Computing, Vienna, Austria. ISBN 3-900051-07-0, URL http://www.R-project.org.

Schulla, J. & Jasper, K. (2007). Model Description WaSiM-ETH. Technical report, ETH Zürich, 181 pp.

Zaman, M.A., Rahman, A. & Haddad, K. (2012). Regional flood frequency analysis in arid regions. A case study for Australia. J. Hydrol., 475, 74-83.

Appendix I - Identification of homogeneous groups of catchments obtained with the ROI technique and associated growth curves
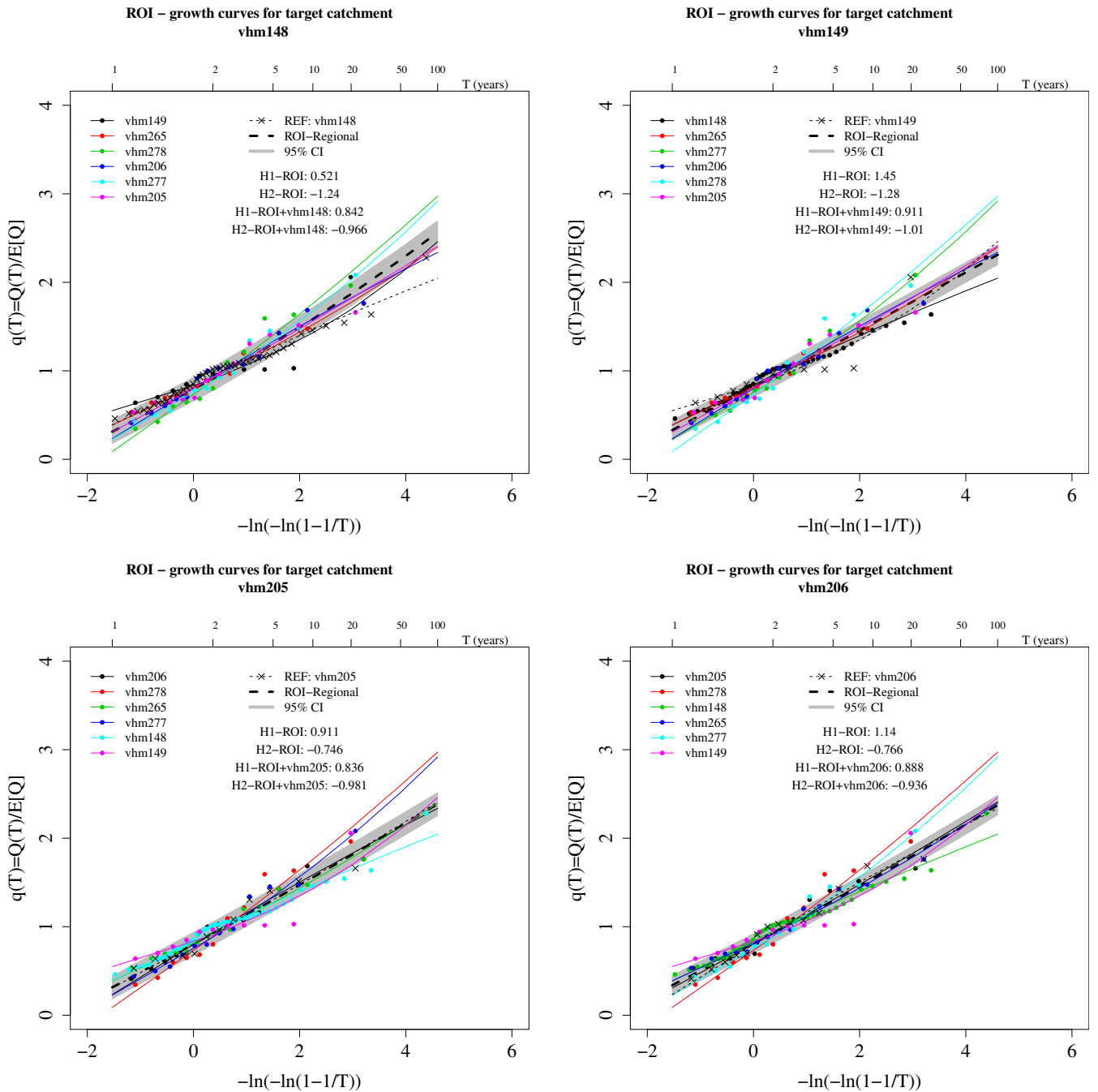
Figure I.1. Homogeneous groups of catchments identified with the ROI technique, associated to vhm148 (top-left), vhm149 (top-right), vhm205 (bottom-left), vhm206 (bottom-right) and corresponding regional and individual growth curves.
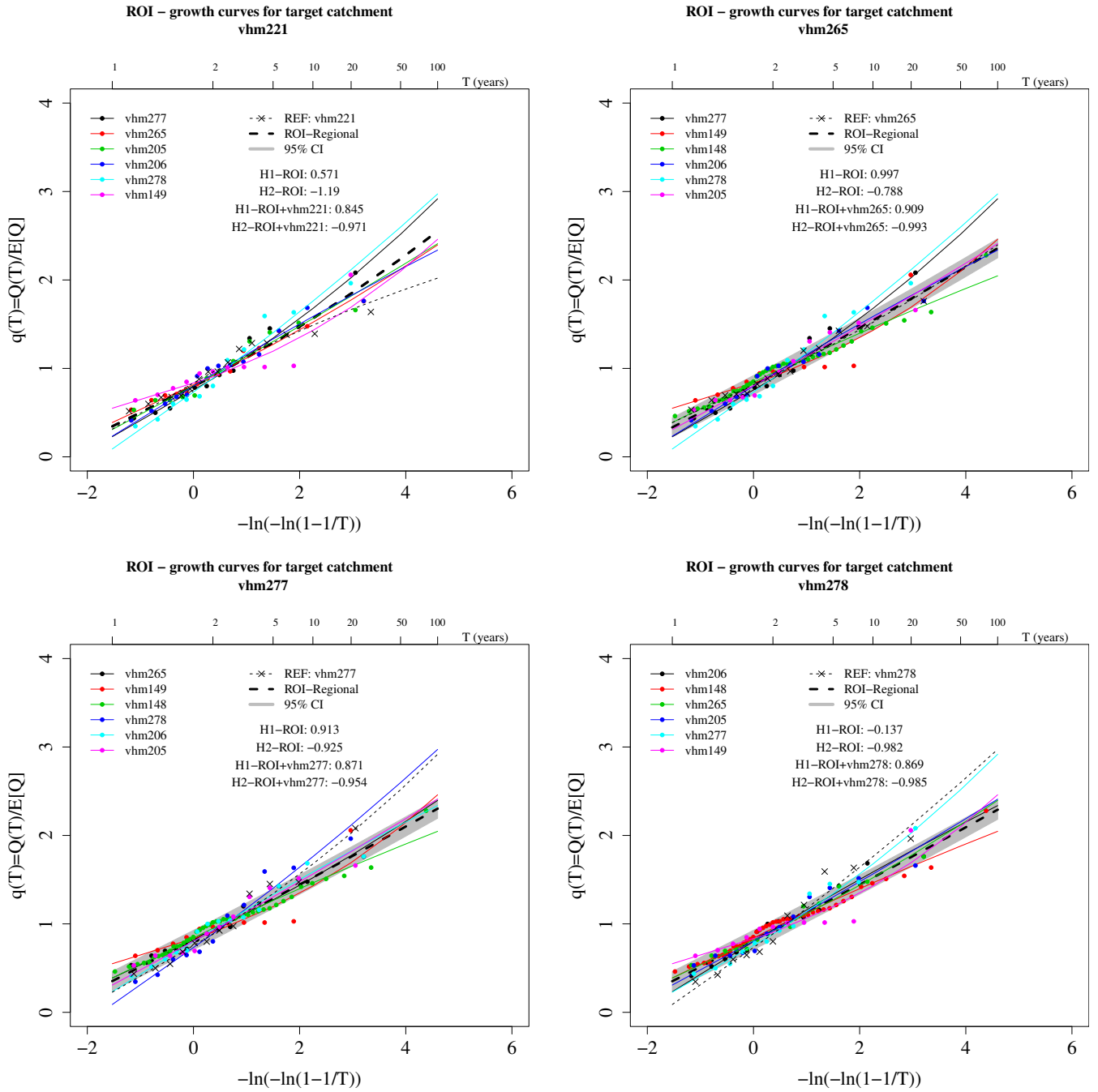
Figure I.2. Homogeneous groups of catchments identified with the ROI technique, associated to vhm221 (top-left), vhm265 (top-right), vhm277 (bottom-left), vhm278 (bottom-right) and corresponding regional and individual growth curves.

Appendix II - WaSiM daily flow simulations: Best run verification for the calibration and validation periods
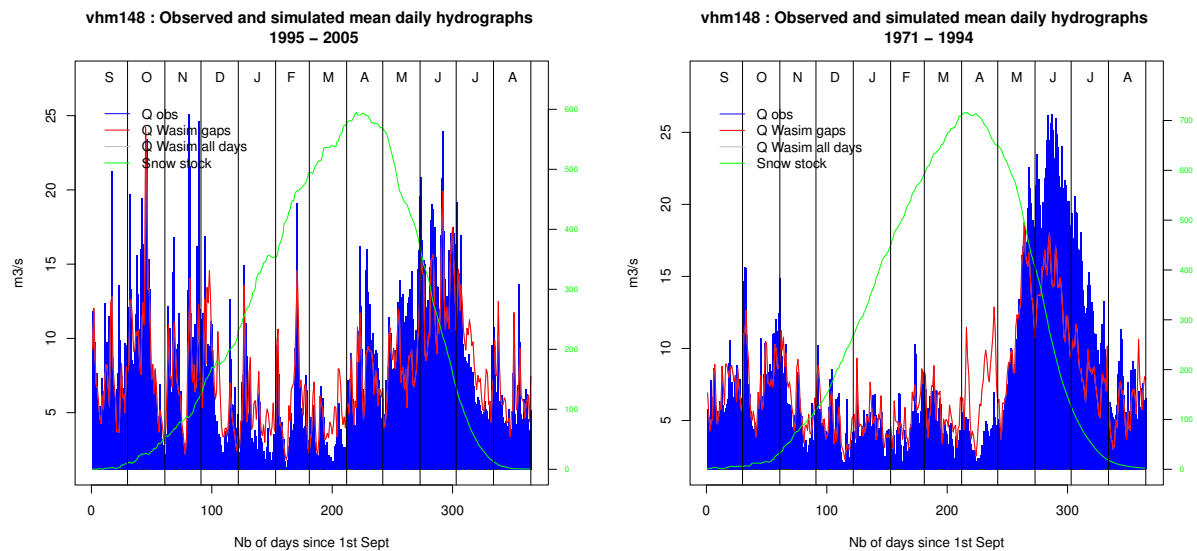
Figure II.1. vhm148: Streamflow seasonality in the calibration period (left), and validation period (right).
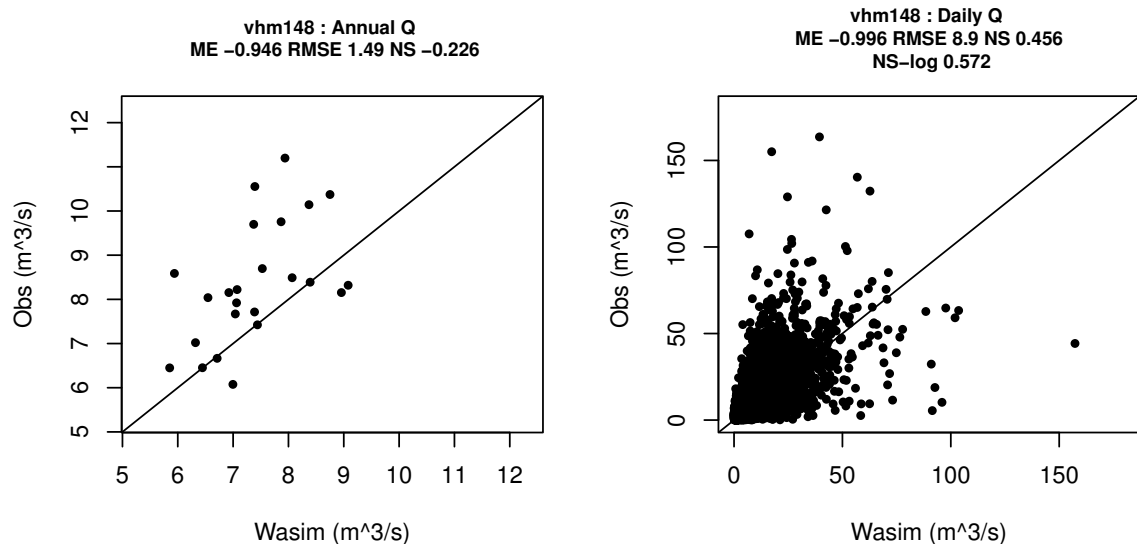
Figure II.2. vhm148: Observed vs. simulated streamflow in the validation period. Annual streamflow (left) and daily streamflow (right).
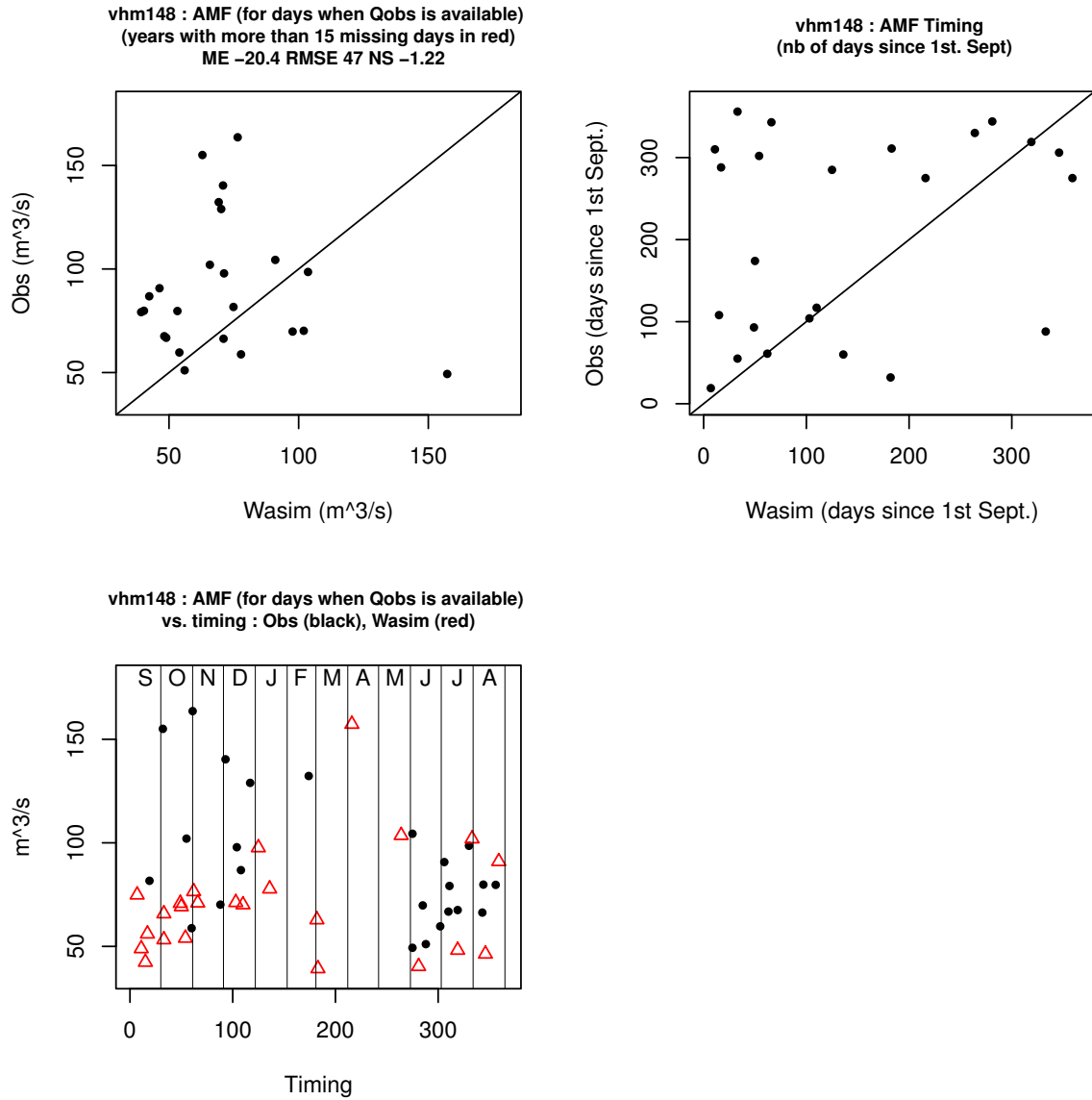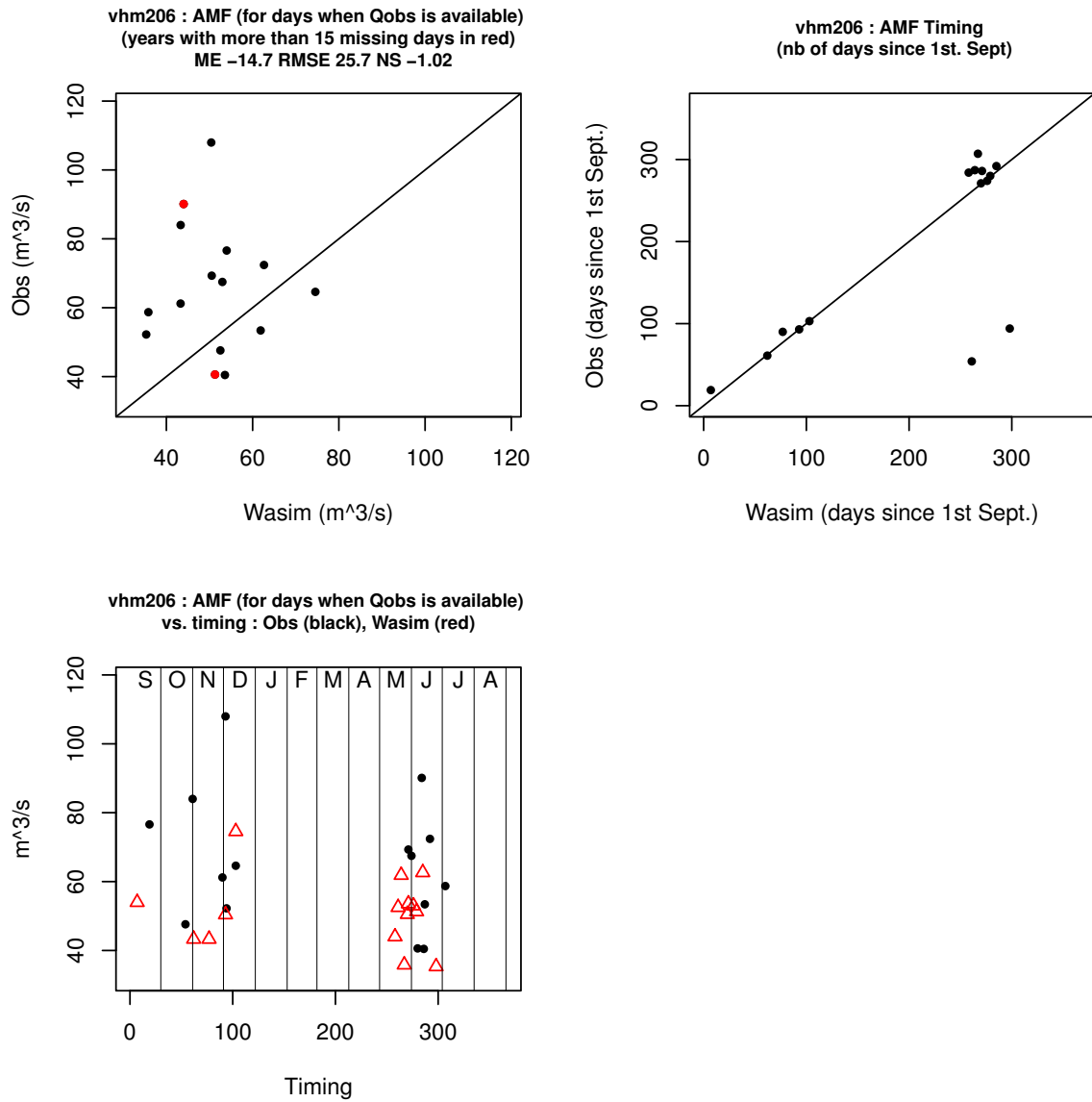
Figure II.3. vhm148: Observed vs. simulated annual maximum flow (AMF) in the validation period (top-left). Observed vs. WaSiM AMF time of occurrence (top-right). AMF vs. time of occurrence (Obs:black circles, WaSiM: red triangles) (bottom-left).
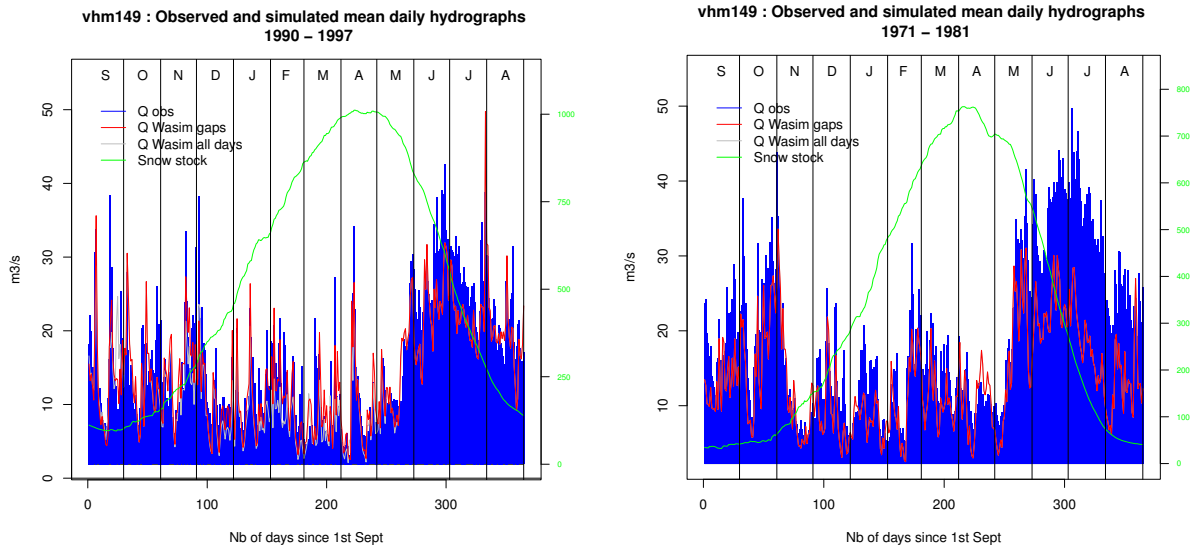
Figure II.4. vhm149: Streamflow seasonality in the calibration period (left), and validation period (right).
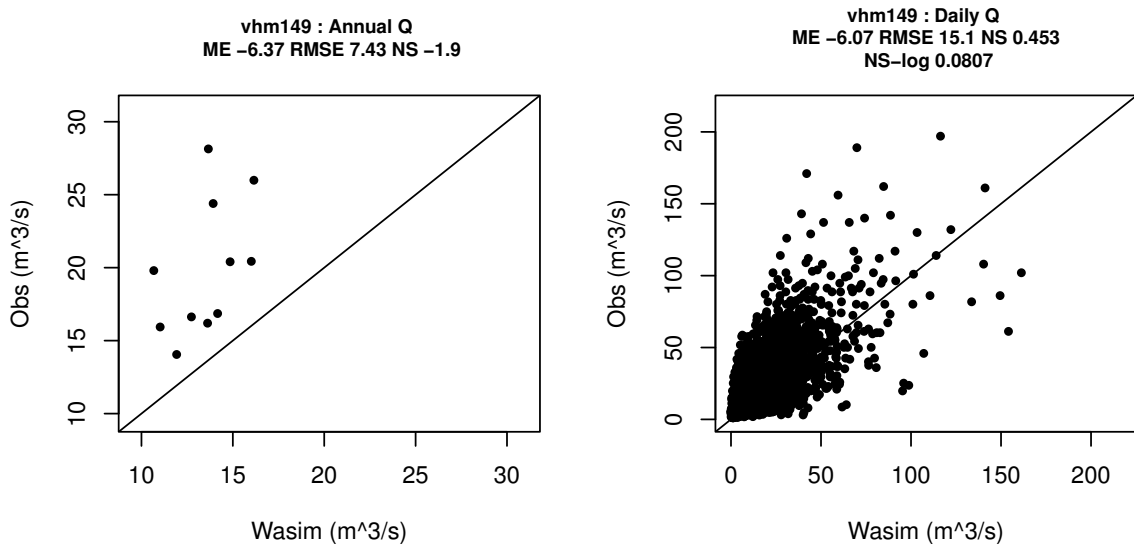
Figure II.5. vhm149: Observed vs. simulated streamflow in the validation period. Annual streamflow (left) and daily streamflow (right).
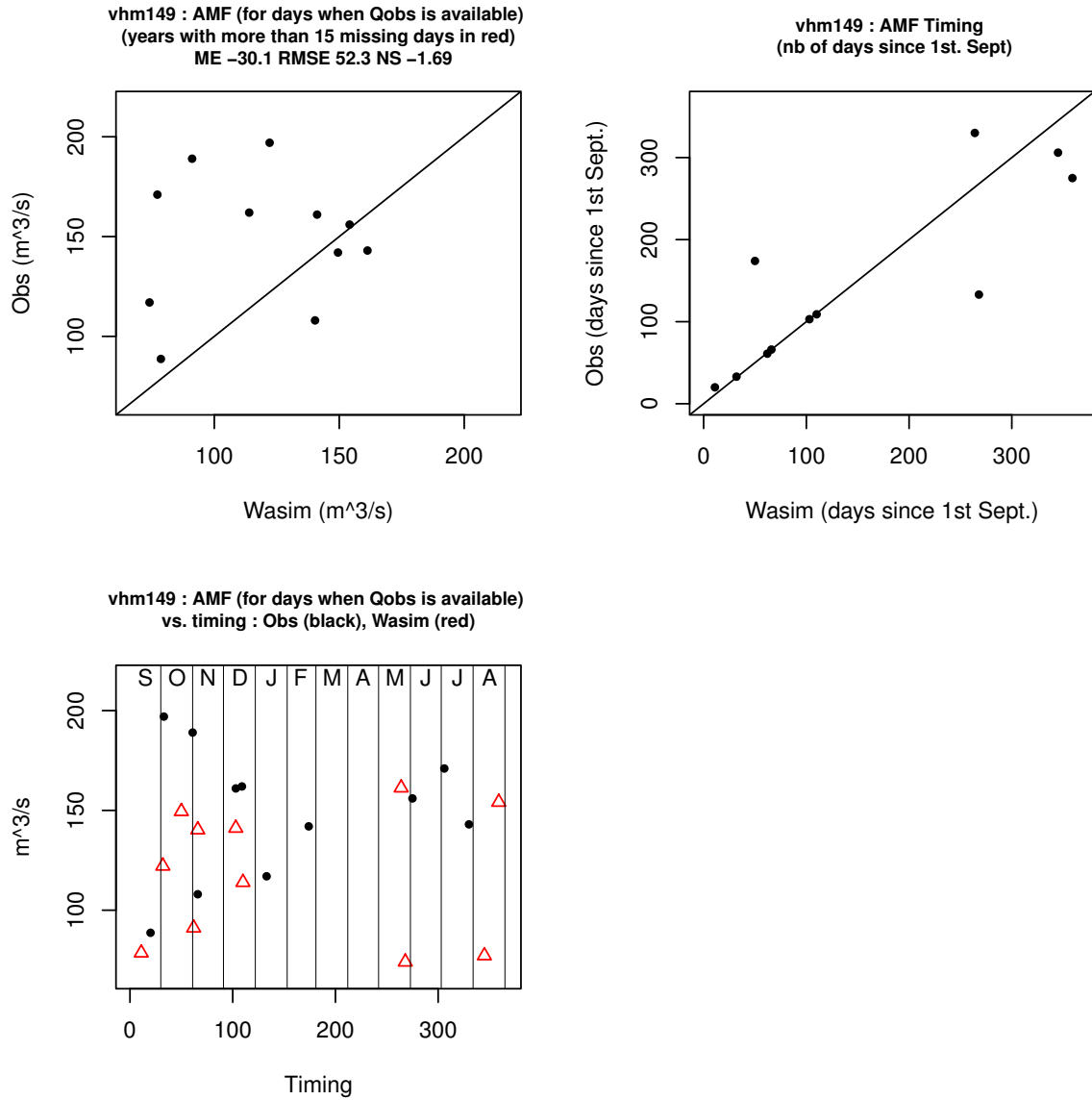
*Figure II.6. vhm149: Observed vs. simulated annual maximum flow (AMF) in the valida-
tion period (top-left). Observed vs. WaSiM AMF time of occurrence (top-right). AMF vs.
time of occurrence (Obs:black circles, WaSiM: red triangles) (bottom-left).*
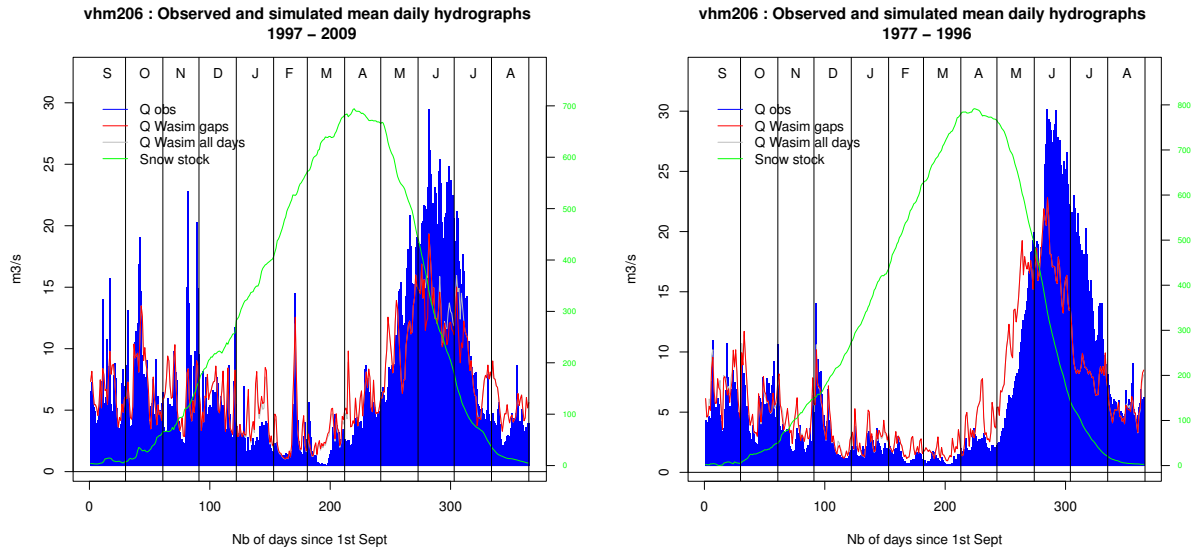
Figure II.7. vhm206: Streamflow seasonality in the calibration period (left), and validation period (right).
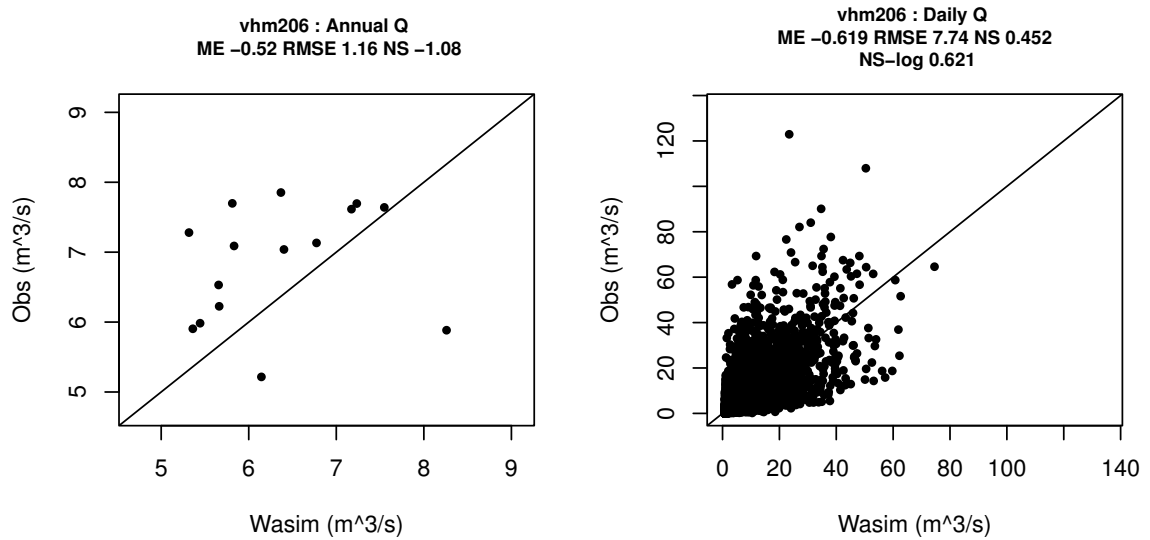
Figure II.8. vhm206: Observed vs. simulated streamflow in the validation period. Annual streamflow (left) and daily streamflow (right).

Figure II.9. vhm206: Observed vs. simulated annual maximum flow (AMF) in the valida-tion period (top-left). Observed vs. WaSiM AMF time of occurrence (top-right). AMF vs. time of occurrence (Obs:black circles, WaSiM: red triangles) (bottom-left).

Appendix III - Instantaneous index flood $\mu_i(D = 0)$, flood frequency distribution and growth curves, derived by QDF modelling of WaSiM daily flow simulations

QDF WaSiM−vhm148
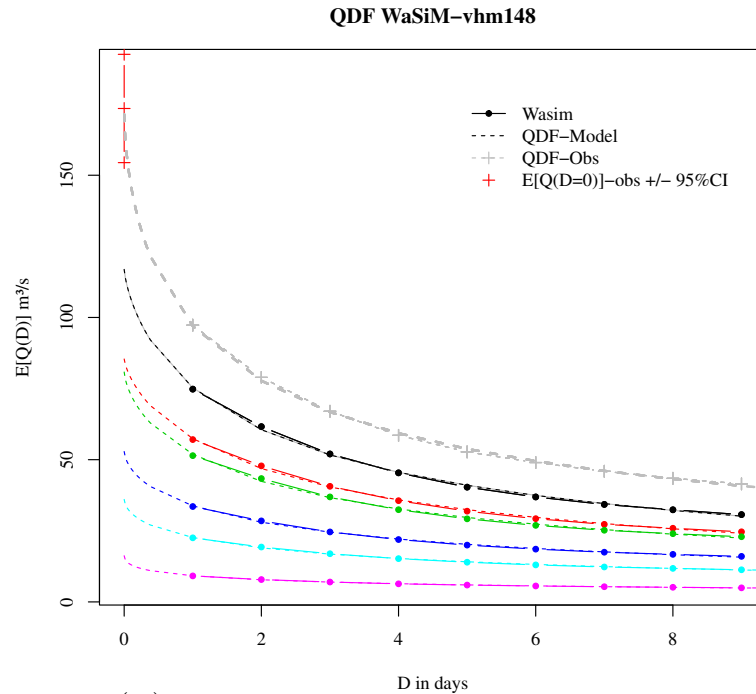
Figure III.1. vhm148: $\mu_i(D)$ vs. D. Grey lines correspond to QDF model derived from AMF observations. Black lines correspond to QDF model derived from WaSiM simulations at gauging station vhm148. Coloured lines correspond to QDF models derived from WaSiM simulations on sub-catchments (see Fig. 7).
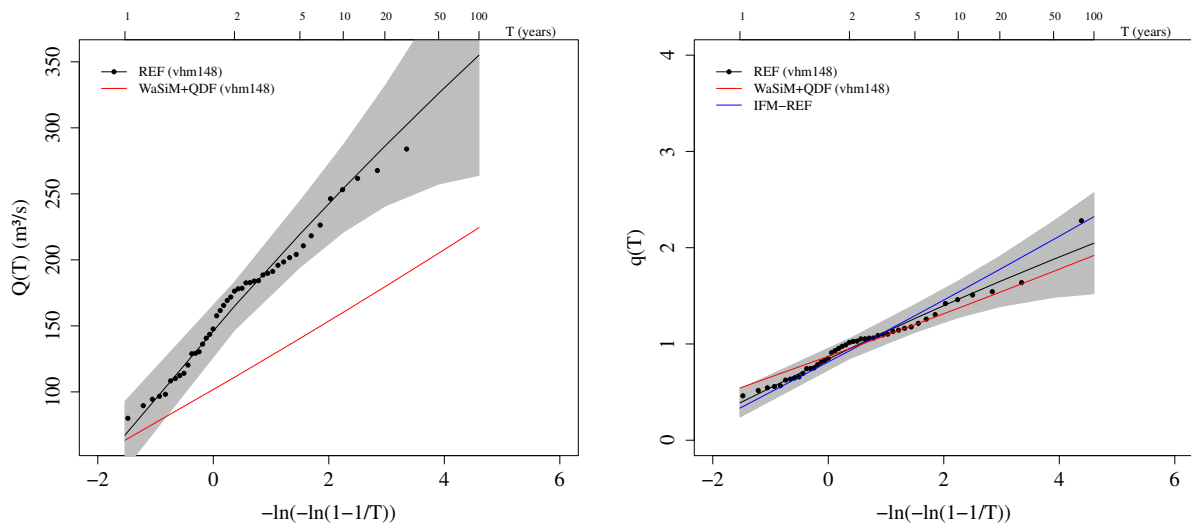
Figure III.2. vhm148: AMF frequency distribution, $Q(D = 0, T)$ vs. T, (left). Growth curves, $q(D = 0, T)$ vs. T, (right). Grey shaded region corresponds to the reference 95% CI. IFM-REF=IFM-CLU where $\mu_i(D = 0)$ is estimated by the arithmetic mean of the observed AMF sample at vhm148.

QDF WaSiM−vhm149
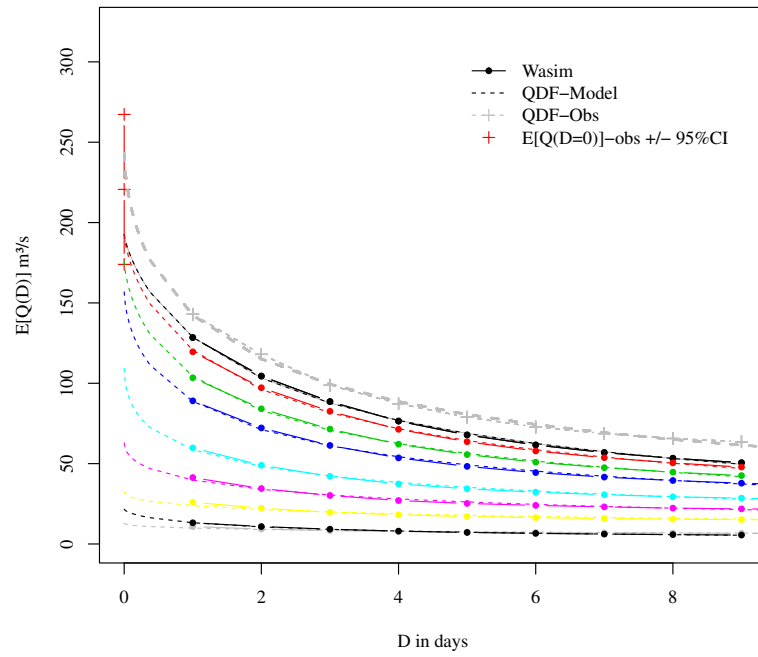
Figure III.3. As Fig. III-1 but for vhm149.
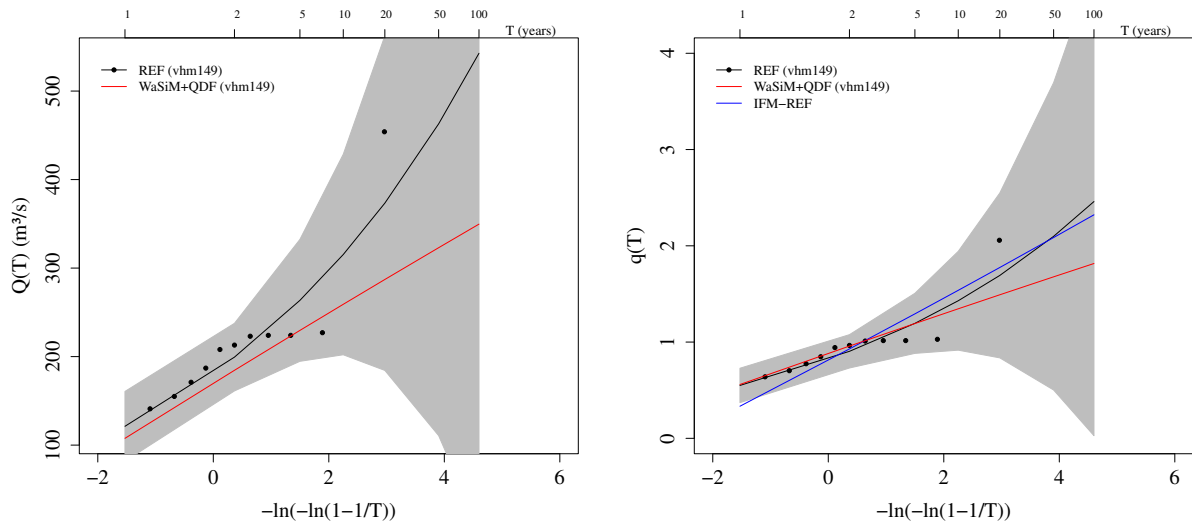
Figure III.4. As Fig. III-2 but for vhm149.
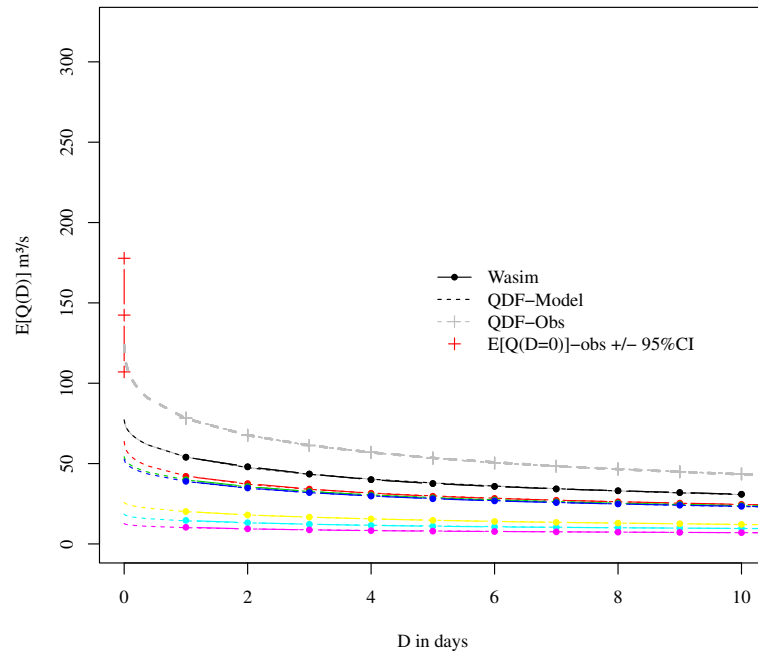
QDF WaSiM−vhm206

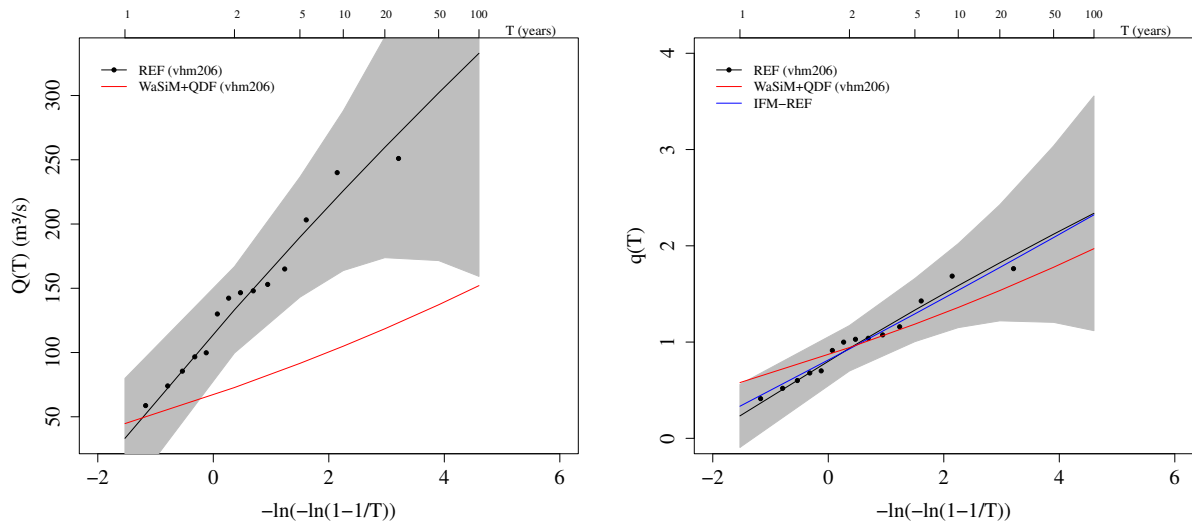*Figure III.5. As Fig. III-1 but for vhm206*

Figure III.6. As Fig. III-2 but for vhm206

43

Appendix IV - Estimated flood frequency distributions at target sites treated as ungauged, using the best IFM for each set
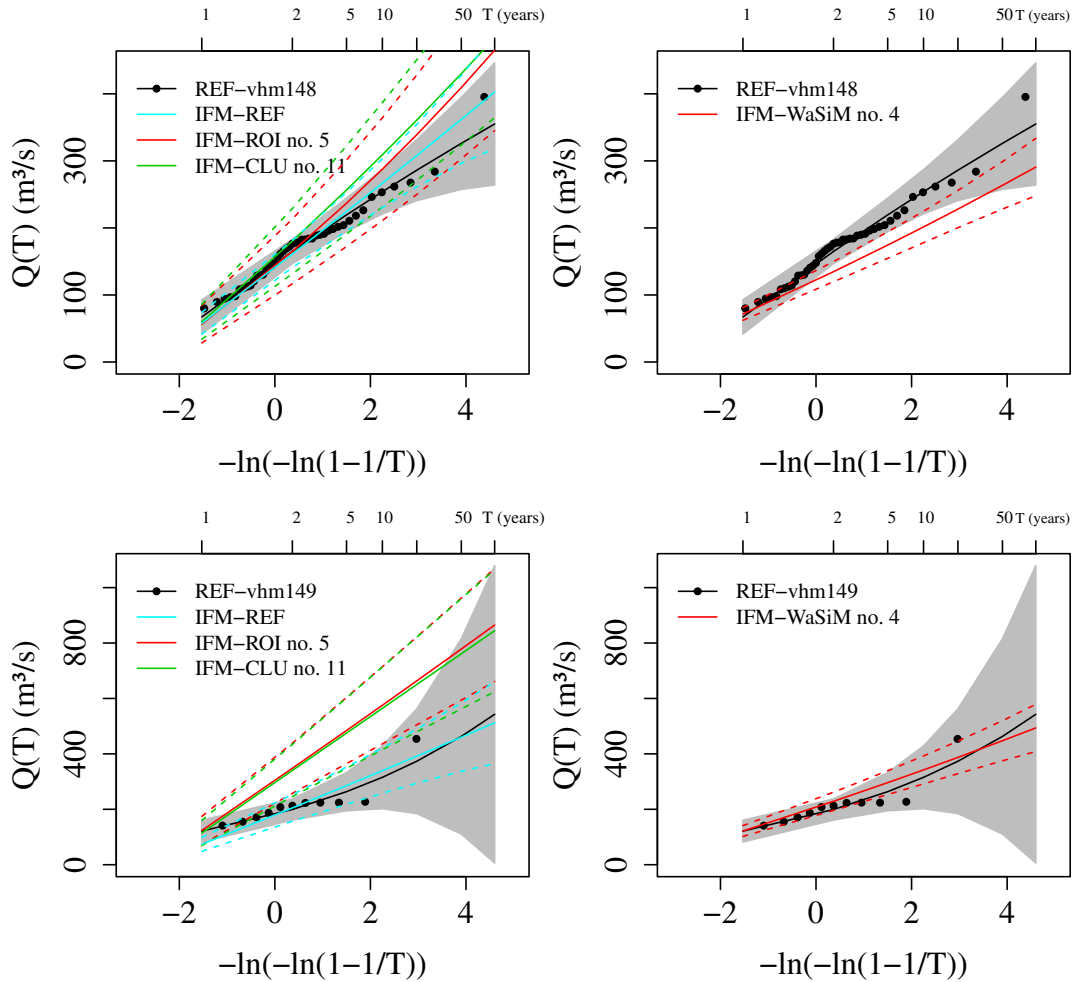

Figure IV.1. AMF frequency distribution ($Q(D = 0, T)$ vs. T) at target sites treated as ungauged, using best IFM-CLU and IFM-ROI (left) and IFM-WaSiM (right): vhm148 (top) and vhm149 (bottom). Grey shaded region corresponds to the reference 95% CI. Coloured dashed lines correspond to the IFM-based 95% CI (See Crochet, 2012a). IFM-REF=IFM-CLU where $\mu_i(D = 0)$ is estimated by the arithmetic mean of the observed AMF sample at target site. For IFM-WaSiM, hydrological modelling uncertainties and QDF modelling uncertainties are not taken into account for the calculation of the CI.
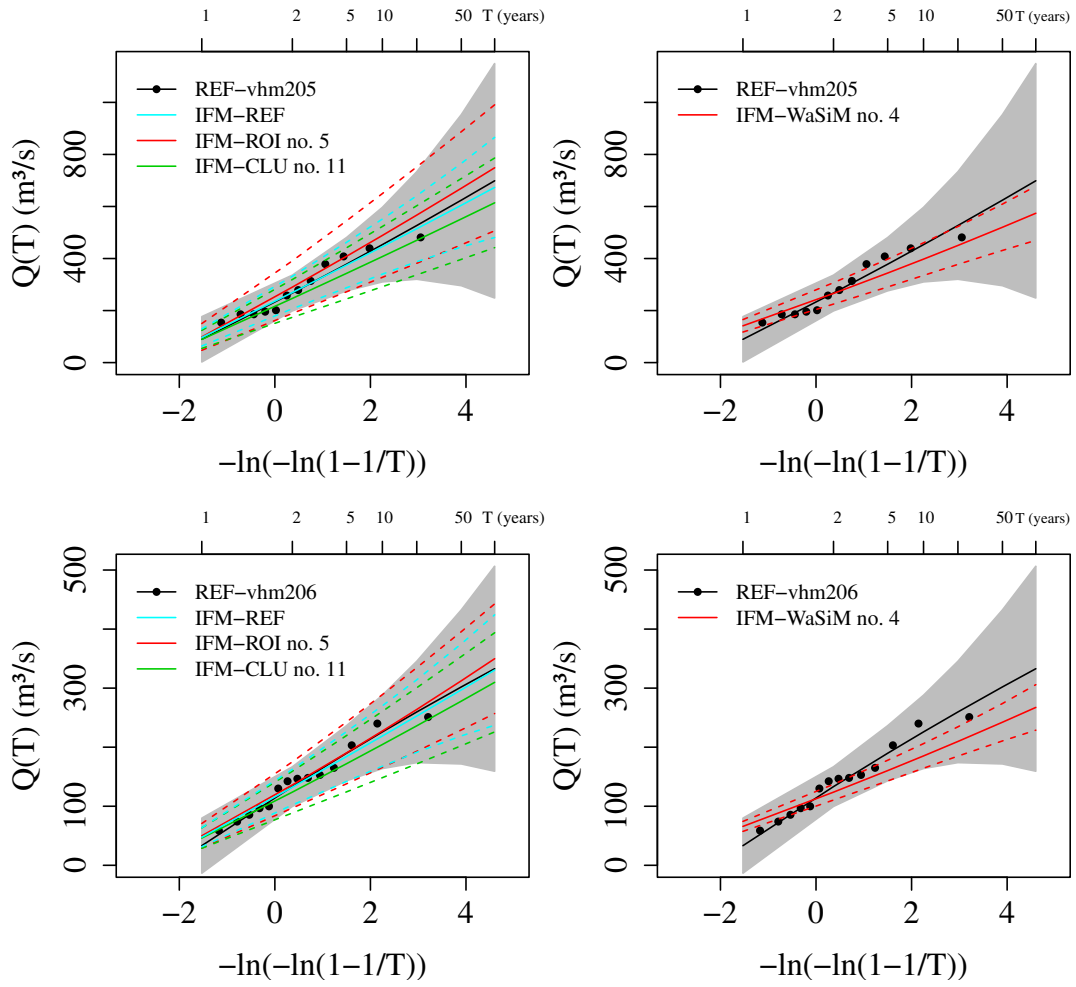
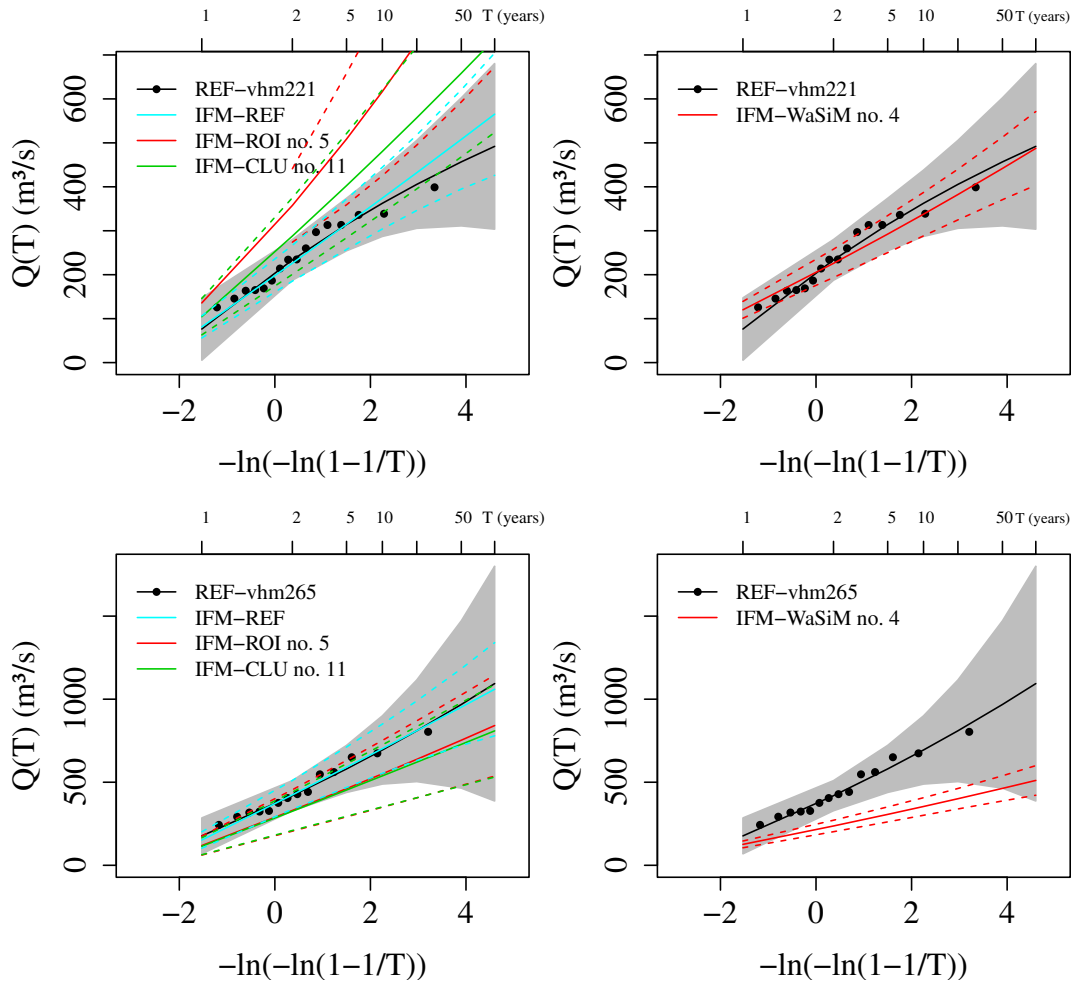*Figure IV.2. As Fig IV-1 but for vhm205 (top) and vhm206 (bottom).*

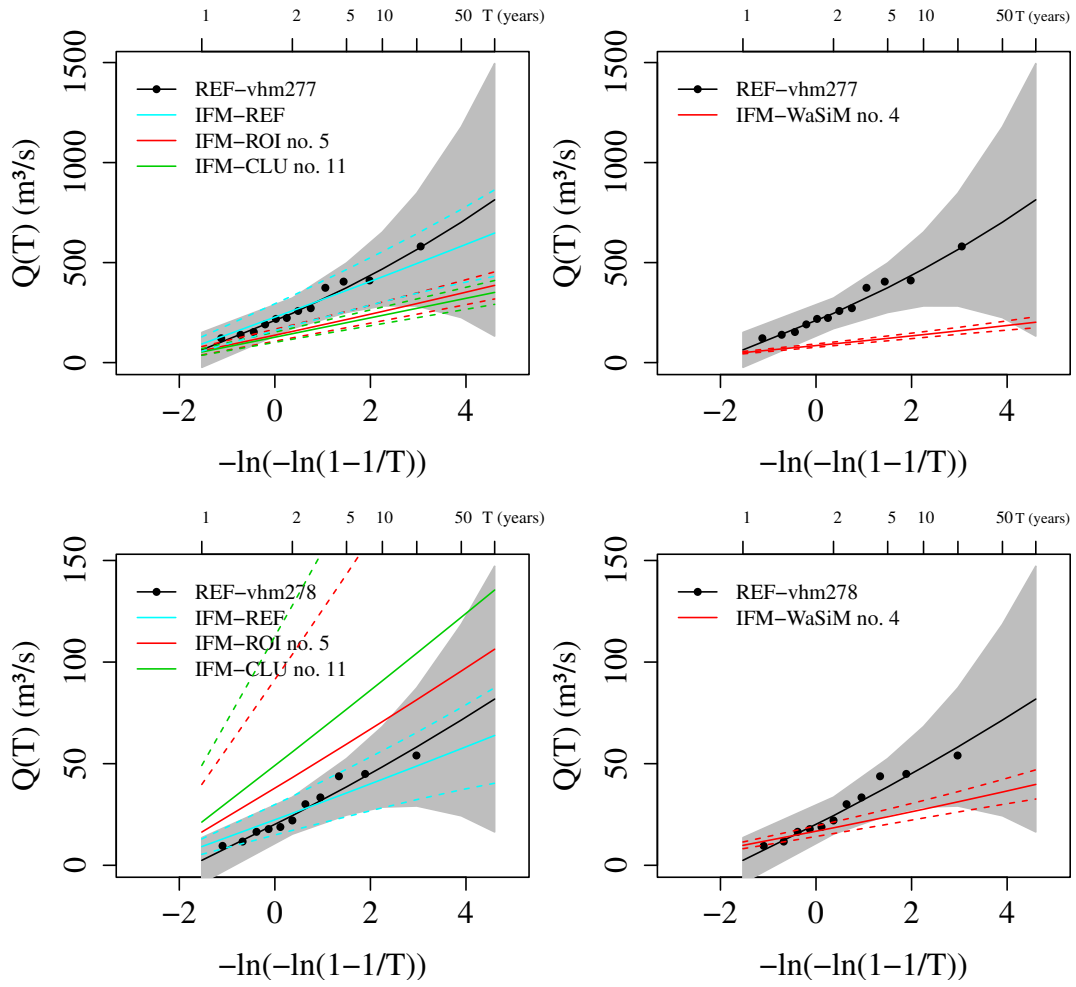*Figure IV.3. As Fig IV-1 but for vhm221 (top) and vhm265 (bottom).*

Figure IV.4. As Fig IV-1 but for vhm277 (top) and vhm278 (bottom).